

## Article

# The Influence of Variations in Synthesis Conditions on the Phase Composition, Strength and Shielding Characteristics of $\text{CuBi}_2\text{O}_4$ Films

Dauren B. Kadyrzhanov <sup>1</sup>, Medet T. Idinov <sup>2</sup>, Dmitriy I. Shlimas <sup>1,3,\*</sup>  and Artem L. Kozlovskiy <sup>1,3</sup> 

<sup>1</sup> Engineering Profile Laboratory, L.N. Gumilyov Eurasian National University, Satpayev St., Astana 010008, Kazakhstan; kadyrzhanov.d@enu.edu.kz (D.B.K.); kozlovskiy.a@inp.kz (A.L.K.)

<sup>2</sup> Department of Technical Physics and Thermal Power Engineering, NJSK Shakarim University of Semey, Shygayev St., Semipalatinsk 071400, Kazakhstan; medet@nuamed.kz

<sup>3</sup> Laboratory of Solid State Physics, The Institute of Nuclear Physics, Ibragimov St., Almaty 050032, Kazakhstan

\* Correspondence: shlimas@inp.kz

**Abstract:** This paper presents the results of the influence of variation of the synthesis conditions of  $\text{CuBi}/\text{CuBi}_2\text{O}_4$  films with a change in the applied potential difference, as well as a change in electrolyte solutions (in the case of adding cobalt or nickel sulfates to the electrolyte solution) on changes in the phase composition, structural parameters and strength characteristics of films obtained using the electrochemical deposition method. During the experiments, it was found that, in the case of the addition of cobalt or nickel to the electrolyte solutions, the formation of films with a spinel-type tetragonal  $\text{CuBi}_2\text{O}_4$  phase is observed. In this case, a growth in the applied potential difference leads to the substitution of copper with cobalt (nickel), which in turn leads to an increase in the structural ordering degree. It should be noted that, during the formation of  $\text{CuBi}/\text{CuBi}_2\text{O}_4$  films from solution–electrolyte №1, the formation of the  $\text{CuBi}_2\text{O}_4$  phase is observed only with an applied potential difference of 4.0 V, while the addition of cobalt or nickel sulfates to the electrolyte solution results in the formation of the tetragonal  $\text{CuBi}_2\text{O}_4$  phase over the entire range of the applied potential difference (from 2.0 to 4.0 V). Studies have been carried out on the strength and tribological characteristics of synthesized films depending on the conditions of their production. It has been established that the addition of cobalt or nickel sulfates to electrolyte solutions leads to an increase in the strength of the resulting films from 20 to 80%, depending on the production conditions (with variations in the applied potential difference). During the studies, it was established that substitution of copper with cobalt or nickel in the composition of  $\text{CuBi}_2\text{O}_4$  films results in a rise in the shielding efficiency of low-energy gamma radiation by 3.0–4.0 times in comparison with copper films, and 1.5–2.0 times for high-energy gamma rays, in which case the decrease in efficiency is due to differences in the mechanisms of interaction of gamma quanta, as well as the occurrence of secondary radiation as a result of the formation of electron–positron pairs and the Compton effect.

**Keywords:** radiation shielding; protective materials; thin films; electrochemical synthesis; substitution effect



**Citation:** Kadyrzhanov, D.B.; Idinov, M.T.; Shlimas, D.I.; Kozlovskiy, A.L. The Influence of Variations in Synthesis Conditions on the Phase Composition, Strength and Shielding Characteristics of  $\text{CuBi}_2\text{O}_4$  Films. *Crystals* **2024**, *14*, 453. <https://doi.org/10.3390/cryst14050453>

Academic Editor: Sven L. M. Schroeder

Received: 24 March 2024

Revised: 29 April 2024

Accepted: 9 May 2024

Published: 10 May 2024



**Copyright:** © 2024 by the authors. Licensee MDPI, Basel, Switzerland. This article is an open access article distributed under the terms and conditions of the Creative Commons Attribution (CC BY) license (<https://creativecommons.org/licenses/by/4.0/>).

## 1. Introduction

Today, the problem of protection from the negative effects of ionizing radiation on living organisms, as well as microelectronics (operating in conditions of increased background radiation), is one of the most important in the modern world [1–3]. There are many reasons for this; first of all, the increased use of various sources of ionizing radiation (non-natural origin) in various industries (energy, medicine, etc.) leads to an increase in the likelihood of exposure to radiation on living organisms, which can lead to negative consequences, including mutations, diseases and deterioration of health [4,5]. At the same time, artificial sources of ionizing radiation are increasingly used in medicine (X-ray machines, gamma

knives, proton and heavy ion accelerators for the treatment of tumors), which requires increasing the level of protection from exposure to ionizing radiation for personnel who are directly involved in their maintenance and operation, since classical traditional methods of protection in these cases cannot always be used [6,7].

An important role in developments to shield ionizing radiation is also played by work related to the disposal of nuclear waste at nuclear power plants or nuclear test sites, where it is necessary to comply with strict control and safety standards for long-term storage, as well as to minimize the negative impact of ionizing radiation on the environment [8,9]. Among the most effective materials for these purposes are carbide and nitride ceramics, which have high strength and wear resistance, as well as resistance to radiation damage during prolonged exposure and the accumulation of high doses of damage [10–12].

Recently, much attention has been paid to research on the prospects of using thin films or thin-film coatings as shielding protective materials, interest in which is primarily due to the possibility of using them to create local protection of key components of microelectronic devices operating under conditions of exposure to increased background radiation (in spacecraft, satellites or nuclear power plants) [13–15]. Thus, the use of CuBi/CuBi<sub>2</sub>O<sub>4</sub> films as promising materials for protection against the negative effects of electromagnetic radiation was shown in [16,17]. Much attention is paid to composite materials and films consisting of oxide compounds and polymer films as protective shielding materials [18,19]. Interest in such research is due to the possibility of expanding the classes of protective materials, as well as thin, lightweight and sufficiently flexible shields that can be used to protect complex-profile objects. Moreover, these technological solutions are based on technologies for combining light and heavy elements, as well as binding polymer matrices, which serve both as a basis for applied coatings and as matrices in which oxide particles are equally distributed throughout the entire volume [20]. Therefore, for example, in [21], the authors show the prospects for using composite materials based on polymer matrices with oxide nanoparticles placed in them as shielding materials with high shielding efficiency, which are due to the presence of oxides such as WO<sub>3</sub> and Bi<sub>2</sub>O<sub>3</sub>. Also, the use of composite materials in the form of coatings or films is aimed primarily at reducing the cost of production of microelectronic devices for operation in flows of ionizing radiation, for protection against which the classic scheme of duplicating key components is used in order to avoid failures due to radiation damage caused by exposure to ionizing radiation [22,23]. At the same time, the use of these technological solutions makes it possible to solve the issue of protecting key components from the negative effects of ionizing radiation, as well as to reduce the load on the weight and dimensions of microcircuits, which plays a very important role in the case of spacecraft, since transporting each kilogram into orbit requires large amounts of fuel. Thin films play an important role in shielding not only various types of ionizing radiation (gamma, neutron or electron), but also in protecting against electromagnetic influence, which can lead to failures in microelectronic devices along with radiation damage [24,25].

Based on the analysis of the main areas of research in the field of development of shielding materials and their application, the goal of this research was formulated, which is aimed at creating effective shielding materials that can have a positive effect in this direction. The key purpose of this work is to develop a technology for producing composite films based on compounds of copper, bismuth, nickel, cobalt and their oxide compounds such as CuBi/CuBi<sub>2</sub>O<sub>4</sub>, as well as to evaluate their use as shielding materials for protection against the negative effects of ionizing radiation [26,27].

The novelty and relevance of this research is based on the possibility of obtaining new types of high-strength shielding materials based on CuBi/CuBi<sub>2</sub>O<sub>4</sub> with the partial replacement of copper with cobalt or nickel, which can be used to protect against the negative effects of ionizing radiation (gamma and X-rays), and also be used as flexible protective shields for shielding, which have good corrosion resistance and wear resistance (resistance to mechanical stress). The choice as research objects for the development of protective shielding films based on CuBi/CuBi<sub>2</sub>O<sub>4</sub> is due to the high density of these

compounds (about 8.5–8.6 g/cm<sup>3</sup>), comparable to alternative ceramic or glass-like materials based on oxide compounds of tellurium, tungsten, bismuth and lead (the density of these structures varies from 5.0 to 10 g/cm<sup>3</sup>, depending on the number of components in the material and their stoichiometric composition), as well as the possibility of creating protective films with great flexibility, which is due to the polymer matrix being used as a substrate for the synthesized films, which allows them to be used in shielding devices of complex geometry. Moreover, consideration of the possibility of partial replacement of copper in the CuBi<sub>2</sub>O<sub>4</sub> composition with related elements such as nickel, cobalt or iron is due to the possibility of increasing not only the shielding efficiency due to changes in the charge number ( $Z_{\text{eff}}$ ) when replacing copper, but also increasing the strength parameters (hardness, wear resistance, corrosion resistance) due to the formation of a more stable film structure. The choice of nickel and cobalt as components to replace copper is due to their similarity of atomic radii ( $r_{\text{Cu}}$ —128 pm,  $r_{\text{Co}}$ —125 pm,  $r_{\text{Ni}}$ —124 pm), as well as their electrode reduction potentials, which makes it possible to use the method of varying the applied potential difference to vary the ratio of elements in the composition of the films. The use of nickel and cobalt in electrochemical deposition, meanwhile, has proven itself rather well in order to obtain sufficiently strong and wear-resistant coatings that have higher corrosion resistance rates than copper coatings, which have a tendency for rapid oxidation.

## 2. Materials and Research Methods

### 2.1. Preparation of Solutions–Electrolytes for the Synthesis of Thin Films

The following components were used as initial components for preparing electrolyte solutions: solution–electrolyte №1 to obtain CuBi/CuBi<sub>2</sub>O<sub>4</sub> films—CuSO<sub>4</sub>·5H<sub>2</sub>O (238 g/L), Bi<sub>2</sub>(SO<sub>4</sub>)<sub>3</sub> (10 g/L), H<sub>2</sub>SO<sub>4</sub> (21 g/L); solution–electrolyte №2 to obtain CuBi/CuBi<sub>2</sub>O<sub>4</sub> films with partial substitution of copper by nickel—CuSO<sub>4</sub>·5H<sub>2</sub>O (200 g/L), Co<sub>2</sub>SO<sub>4</sub>·7H<sub>2</sub>O (40 g/L), Bi<sub>2</sub>(SO<sub>4</sub>)<sub>3</sub> (10 g/L), H<sub>2</sub>SO<sub>4</sub> (21 g/L); solution–electrolyte №3 to obtain CuBi/CuBi<sub>2</sub>O<sub>4</sub> films with partial substitution of copper with cobalt—CuSO<sub>4</sub>·5H<sub>2</sub>O (200 g/L), Ni<sub>2</sub>SO<sub>4</sub>·7H<sub>2</sub>O (40 g/L), Bi<sub>2</sub>(SO<sub>4</sub>)<sub>3</sub> (10 g/L), H<sub>2</sub>SO<sub>4</sub> (21 g/L). Solutions–electrolytes were prepared by dissolving all components in given proportions in distilled water, mixing the components using magnetic stirrers at a constant stirring speed (50–100 rpm) and a temperature of 45–50 °C, in order to achieve complete dissolution of all the salts used. The selection of the ratio of components for the preparation of electrolyte solutions was carried out experimentally, the purpose of which was to test the modes of film production and the ability to control the stoichiometric composition of the resulting films. After stirring in order to achieve complete dissolution of all salts, the resulting solutions were kept for two to three hours until they reached room temperature, in order to prevent the influence of temperature factors on the processes of electrochemical reduction in the metal deposit in the form of films on the surface of the substrates.

For the synthesis of films, a PLA cell printed using additive technologies was chosen. The distance between the electrodes was fixed and amounted to 3 cm; for this, the upper electrode was placed on a special platform located at a fixed distance from the lower electrode. Chlorine, a silver electrode, was chosen as a reference electrode, with the help of which the deposition parameters were monitored. The deposition time of the films was fixed and amounted to 20 min. At the same time, it was experimentally established that an increase in deposition time of more than 60 min leads to a decrease in the deposition rate (a decrease in current density was observed), which is due to the depletion of the electrolyte solution over time.

The main method for producing thin films was the electrochemical synthesis method, which is based on the reduction in a metal deposit from aqueous solutions–electrolytes on the surface of the cathode when an electric current passes through the solution–electrolyte. Copper plates of the same area were used as the anode and cathode, varying which makes it possible to obtain films of different sizes. To study the effect of variation in synthesis conditions on the phase composition of the films, the variation range of the applied potential difference was chosen from 2.0 to 4.0 V with a step of 0.5 V, which made it possible to

obtain films with a controlled phase composition, as well as a different ratio of elements, the change in which occurs with varying synthesis conditions. In the case of using solution–electrolyte №1 (without additives), an elevation in the applied potential difference above 4.0 V leads to structural ordering and dominance of the  $\text{CuBi}_2\text{O}_4$  phase over the Cu(Bi) phase (see the example X-ray diffraction patterns of samples obtained using solution–electrolyte №1 in Figure 1). If the applied potential difference increases above 4.0 V when using electrolyte solutions with the addition of cobalt sulfates (solution №2) and nickel sulfates (solution №3), a rapid release of oxygen is observed in the electrochemical cell, which leads to uneven deposition associated with partial overlap of the cathode surface. Based on this, the range of applied potential differences in this experiment was chosen from 2.0 to 4.0 V.

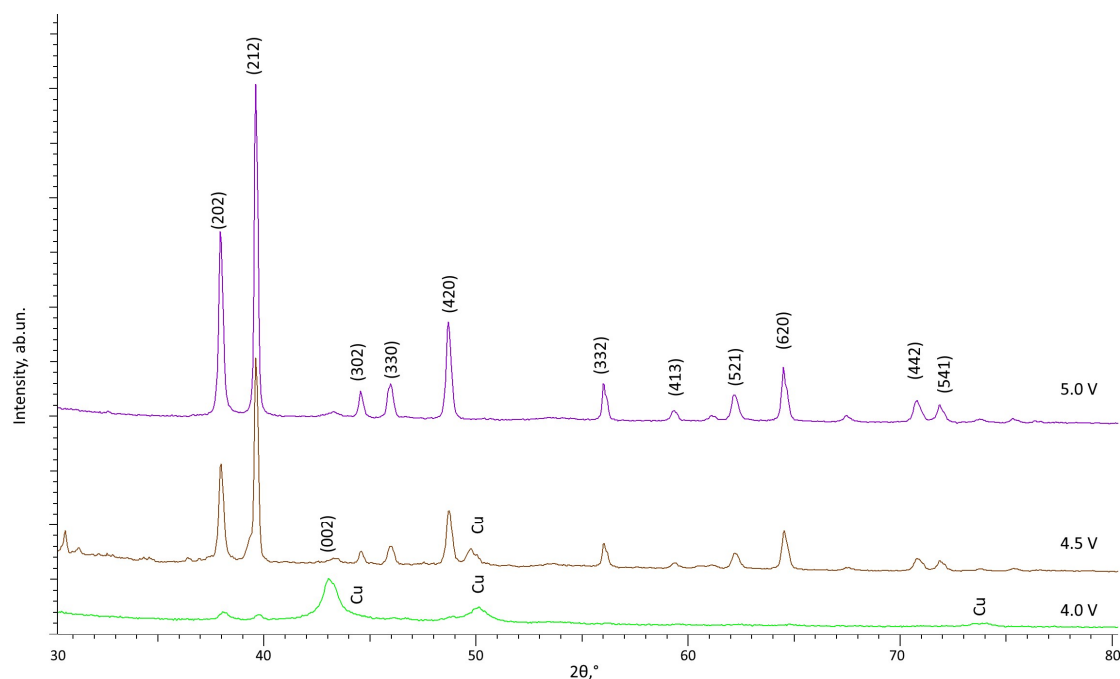


**Figure 1.** Results of a comparative analysis of X-ray diffraction patterns of Cu(Bi)/ $\text{CuBi}_2\text{O}_4$  films obtained at applied potential differences in the range from 4.0 to 5.0 V.

## 2.2. Characterization of the Films under Study

To determine the surface morphology of the resulting thin films depending on variations in synthesis conditions (changes in electrolyte solution, difference in applied potentials), the atomic force microscopy method was used, implemented on a Smart SPM microscope (AIST-NT, Zelenograd, Russia) in semi-contact shooting mode. Based on the data obtained, 3D images of the sample surface were constructed, reflecting changes in surface morphology during film growth (in the case of changes in deposition time), as well as with variations in synthesis conditions (changes in the electrolyte solution and the difference in applied potentials).

Determination of the phase composition of the synthesized films depending on the synthesis conditions (with variations in the applied potential difference, as well as changes in electrolyte solutions) was carried out using the X-ray diffraction method. The recording of X-ray diffraction patterns was carried out on a D8 ADVANCE ECO X-ray diffractometer (Bruker, Karlsruhe, Germany) in the Bragg–Brentano geometry ( $2\theta = 30\text{--}100^\circ$ , with a step of  $0.03^\circ$  and a diffraction pattern acquisition time at a point of 1 s). The determination of the phase composition was carried out by comparative analysis of the position of diffraction lines on the obtained experimental diffraction patterns with card values from the PDF-2 (2016) database, considering possible distortions of the structure (shift in diffraction lines) caused by the deposition process. At the same time, comparison of the obtained data with

the experimental data was carried out when the card (reference) values from the PDF-2 database coincided with the experimental data with an accuracy of about 90%.

Determination of the elemental composition of the film samples under study, depending on the production conditions, was carried out by recording energy-dispersive spectra on a TM3030 scanning electron microscope (SEM) (Hitachi, Tokyo, Japan), equipped with an attachment for energy-dispersive analysis. The accuracy of the measurements was achieved by taking about 10–15 spectra from different areas of the samples, as well as subsequent assessment of the distribution of elements in the composition of the films using the mapping method (determining the equiprobable distribution of elements over large areas of the samples).

Measurements of the optical properties of the synthesized films depending on the production conditions were performed on a SPECORD 250 PLUS UV-Vis spectrophotometer (Analytik Jena, Jena, Germany). The measurements were carried out in the wavelength range from 300 to 1000 nm with a step of 1 nm.

Determination of the strength characteristics of the synthesized films depending on the conditions of their preparation was carried out using the indentation method, implemented using a Duroline M1 microhardness tester (Metkon, Bursa, Turkey). A Vickers diamond pyramid was used as an indenter; the load on the indenter was 10 N, which made it possible to measure the hardness of thin films without the influence of the indenter on the substrate.

Tests to measure the dry friction coefficient, as well as determine the effectiveness of the effect of replacing copper with cobalt or nickel in the composition of films to external mechanical influences, were performed using a UNITEST 750 tribometer (Ducom Instruments, Bengaluru, India). The tests were carried out by successive tests using a ball-shaped indenter, which was applied to the surface under a load of 100 N. The number of friction repetition cycles was 20,000. Based on the obtained tribological test data, the dry friction coefficient (as well as the dynamics of its change depending on the number of cycles of successive tests), as well as the wear profile of coatings, indicating degradation of the film surface depending on their type, were determined.

### 2.3. Determination of Shielding Efficiency

The assessment of the shielding ability of CuBi/CuBi<sub>2</sub>O<sub>4</sub> films in gamma radiation shielding was carried out using the classical scheme of shielding experiments [28,29]. The efficiency of shielding and intensity reduction in gamma radiation was assessed using a standard method for assessing the intensity of recorded gamma radiation with a certain energy at a distance of 10 cm from the source of gamma rays using a NaI detector. Co<sup>57</sup> (130 keV), Cs<sup>137</sup> (660 keV) and Na<sup>22</sup> (1230 keV) were used as sources of gamma quanta, which made it possible to simulate the processes of interaction of gamma rays with matter, including the photoelectric effect, the Compton effect as well as the formation of electron-positron pairs. The shielding efficiency was determined by changes in the spectra of recorded gamma rays before and after shielding. In the case of using thin shielding films, the quality of the spectrum deteriorates sharply, due to a decrease in statistics, as well as a decrease in line intensity. An increase in the statistical spread of points on the spectrum indicates a small number of recorded effects associated with the passage and subsequent interaction of gamma quanta. The shielding efficiency was determined by comparing the intensity values recorded without a protective shield and using protective shields made of synthesized films.

## 3. Results and Discussion

### 3.1. The Influence of Variations in Solutions–Electrolytes on Changes in the Phase Composition and Structural Parameters of Synthesized CuBi/CuBi<sub>2</sub>O<sub>4</sub> Films

One of the ways to vary the phase composition of films obtained using the electrochemical deposition method is to change the synthesis conditions (variation of the applied potential difference). As is known, a rise in the applied potential difference in the case of two or three-component electrolyte solutions leads to a change in the rate of reduction in

metal ions in the solution, which in turn leads to a change in the elemental composition of the resulting structures, and as a consequence the possibility of changing the phase composition due to the structural formation of films from various elements. In this case, the dominance of the reduction rate (reduction potential) of metal ions from aqueous solutions–electrolytes can lead to the dominance of one of the elements in the resulting structures which, under certain conditions or concentrations, can lead to the formation of new structural elements in the form of inclusions of new phases, or a complete phase transformation of the resulting films. The most reliable method for determining phase and structural changes in films is the X-ray diffraction method, the use of which makes it possible to obtain data not only on phase changes in films when varying the conditions for their production, but also to determine the influence of variations in the applied potential difference (as a consequence, changes in the rate of reduction in metal ions) on the structural parameters of the resulting films and the structural ordering degree.

Figure 2a shows X-ray diffraction patterns of the studied samples of CuBi/CuBi<sub>2</sub>O<sub>4</sub> films obtained from solution–electrolyte №1, with variation in the applied potential difference, the changing of which makes it possible to increase the deposition rate by changing the rate of reduction in metal deposits from sulfuric acid aqueous solutions.

According to the assessment of the general appearance of the presented X-ray diffraction patterns of the studied samples, it can be concluded that a change in the applied potential difference leads to two types of structural changes: (1) a change in the structural ordering degree, expressed in a change in the shape of the diffraction maxima, as well as a change in their intensity (texturing effect); (2) a change in the phase composition of the films, which manifests itself due to the appearance of new diffraction reflections in diffraction patterns at high potential differences. At the same time, the ratio of the intensities of diffraction reflections and background radiation indicates the polycrystalline structure of the resulting films, as well as a fairly high degree of structural ordering (crystallinity degree) of the films, a change in which is observed with variations in synthesis conditions (changes in the applied potential difference).

The general appearance of the presented diffraction patterns, depending on changes in synthesis conditions (with variations in the difference in applied potentials), indicates not only changes in the structural ordering degree (expressed in changes in the shape and intensity of diffraction reflections), but also the processes of phase transformations that appear at applied potential differences above 3.0 V. In the case of applied potential differences from 2.0 to 3.0 V, the main positions of the diffraction reflections presented in the X-ray diffraction patterns correspond to the cubic phase of Cu (PDF-00-004-0836), the formation of which is due to the processes of electrochemical reduction in the metal deposit, as well as the potential for the reduction in copper from sulfuric acid aqueous solutions–electrolytes [30,31]. In this case, the shape and angular position of the diffraction reflections indicate a deformation distortion of the crystal lattice of the tensile type (shift of reflections to the region of small angles), which can be explained by the effect of partial substitution of copper ions by bismuth ions at the crystal lattice sites, the ionic radius of which (1.2 Å) is significantly larger than the ionic radius of copper (0.98 Å). In this case, the shift in the position of the diffraction reflections relative to the initial position (determined for samples of CuBi/CuBi<sub>2</sub>O<sub>4</sub> films obtained at a potential difference of 2.0 V) can be explained by an increase in the bismuth content in the films, which is observed according to energy dispersion analysis data (see results presented in Figure 2a). Also, changes in crystal lattice parameters (their increase) are evidenced by the data presented in Table 1, which were determined using the Nelson–Taylor technique, used to estimate structural parameters by selecting a certain number of approximating functions when analyzing the shape and position of diffraction reflections [32]. At the same time, in the case of an increase in the applied potential difference from 2.0 to 3.5 V, not only a change in the shape of the main diffraction reflections is observed, indicating the structural ordering degree, but also the appearance of a texture effect, which is most pronounced for film samples obtained at potential differences of 3.0–3.5 V, for which an increase in the intensity of the

diffraction reflection is observed at the angular position of  $2\theta = 74.0\text{--}74.5^\circ$ , comparable in magnitude to the intensity of the diffraction reflection at  $2\theta = 43.0\text{--}43.5^\circ$ . This change in the intensities of diffraction reflections with increasing difference in applied potentials is due to the fact that the formation of grains in the film structure occurs along two selected textural directions, which indicates the occurrence of the effect of texture misorientation of grains, which manifests itself for nanostructured materials obtained by electrochemical deposition [33,34].

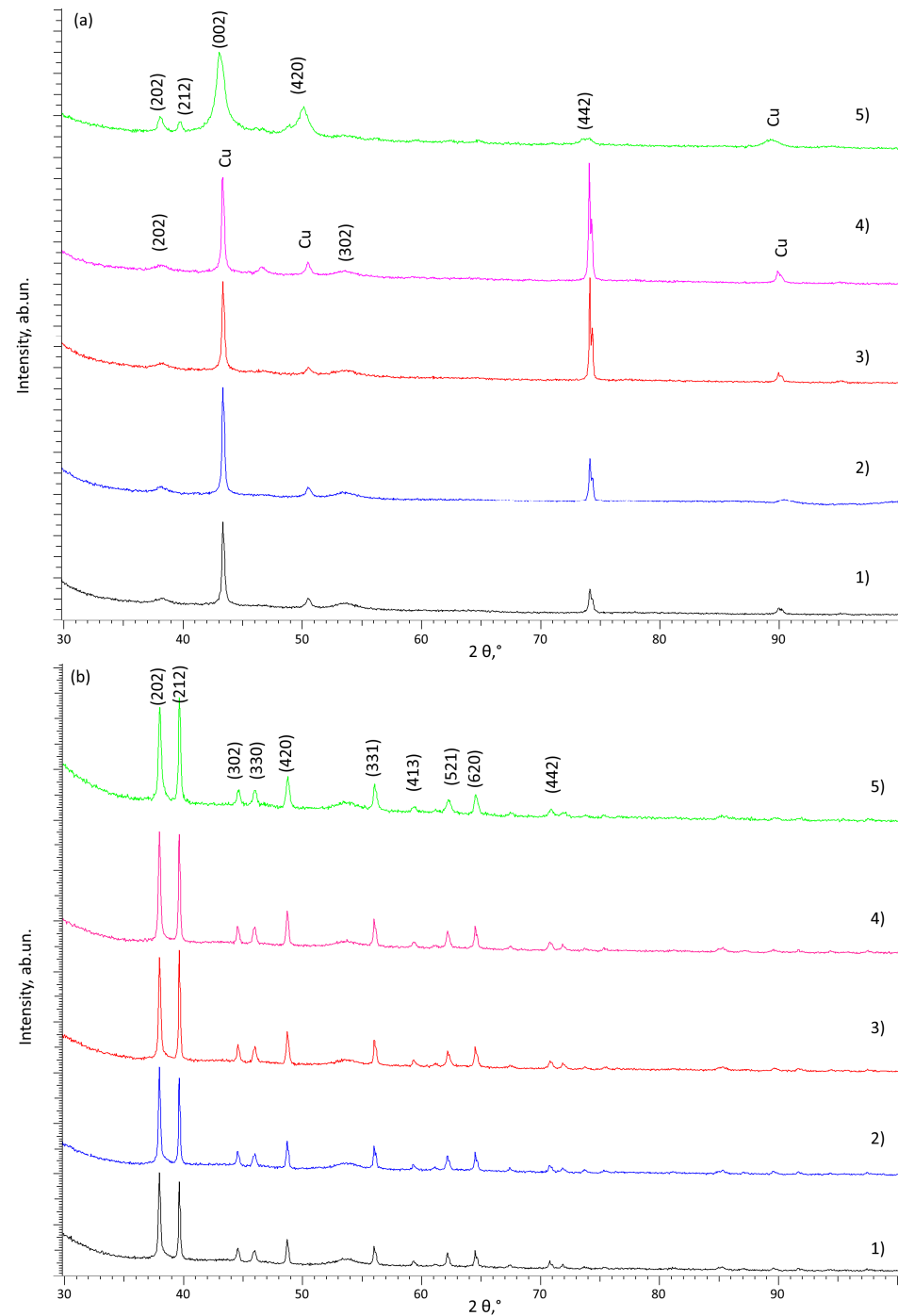
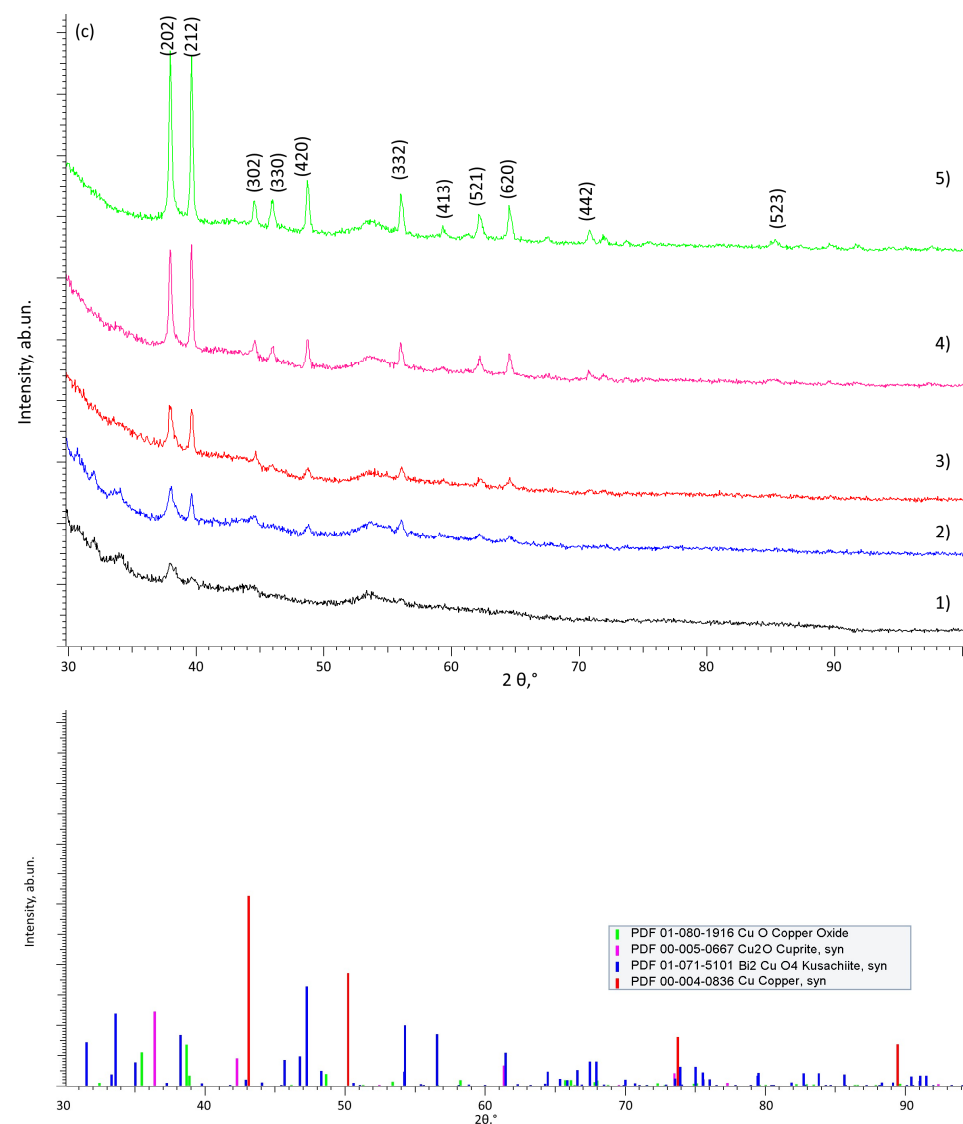


Figure 2. Cont.



**Figure 2.** Results of X-ray diffraction of the studied samples of films obtained using the electrochemical deposition method with variation in the applied potential difference: (1) = 2.0 V, (2) = 2.5 V, (3) = 3.0 V, (4) = 3.5 V, and (5) = 4 V: (a) when using the electrolyte composition to obtain CuBi/CuBi<sub>2</sub>O<sub>4</sub> films; (b) when using the electrolyte composition to obtain Cu(Co)Bi<sub>2</sub>O<sub>4</sub> films; (c) when using the electrolyte composition to obtain Cu(Ni)Bi<sub>2</sub>O<sub>4</sub> films.

Figure 3 demonstrates the mapping results of the film samples under study depending on the type of electrolyte solution used, which reflects the isotropic distribution of elements in the film composition over the surface. The figure also reveals data on the morphological features of the synthesized films, found using the scanning electron microscopy method. The overall appearance of the data presented on the element distribution maps indicates the isotropy of the distribution of elements in the composition of the films. In this case, an alteration in synthesis conditions, in particular, variations in the applied potential difference, leads to the displacement of copper and an increase in the composition of bismuth and oxygen, in the case of using electrolyte solution №1, which has good agreement with the data of X-ray phase analysis. When cobalt or nickel sulfates are added to the electrolyte solution, according to the data presented in Figure 3b,c, it is clear that a growth in the applied potential difference leads to a rise in the content of cobalt or nickel in the composition of the films, while their uniform distribution over the volume is observed, indicating a partial replacement of copper in the composition.

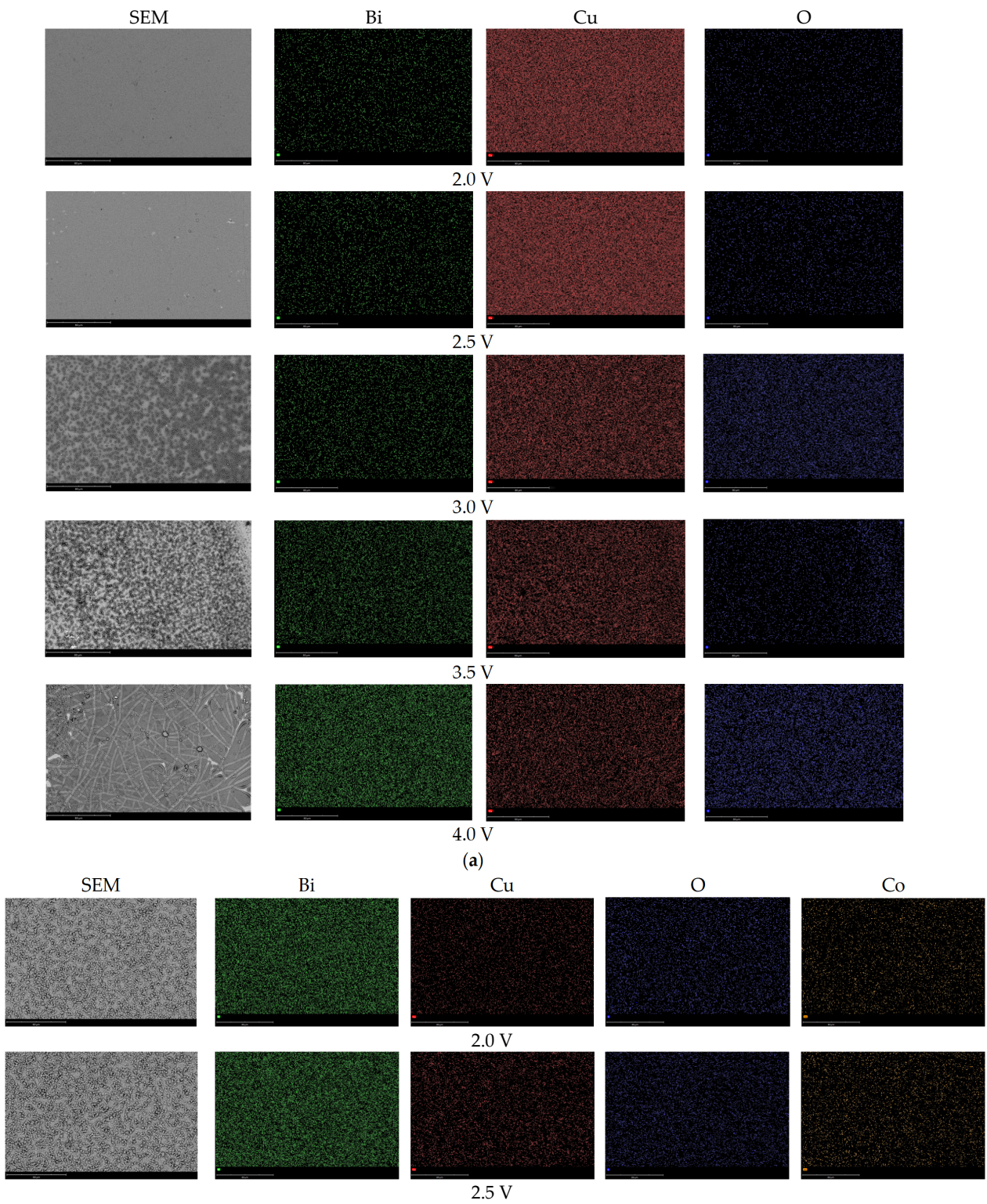
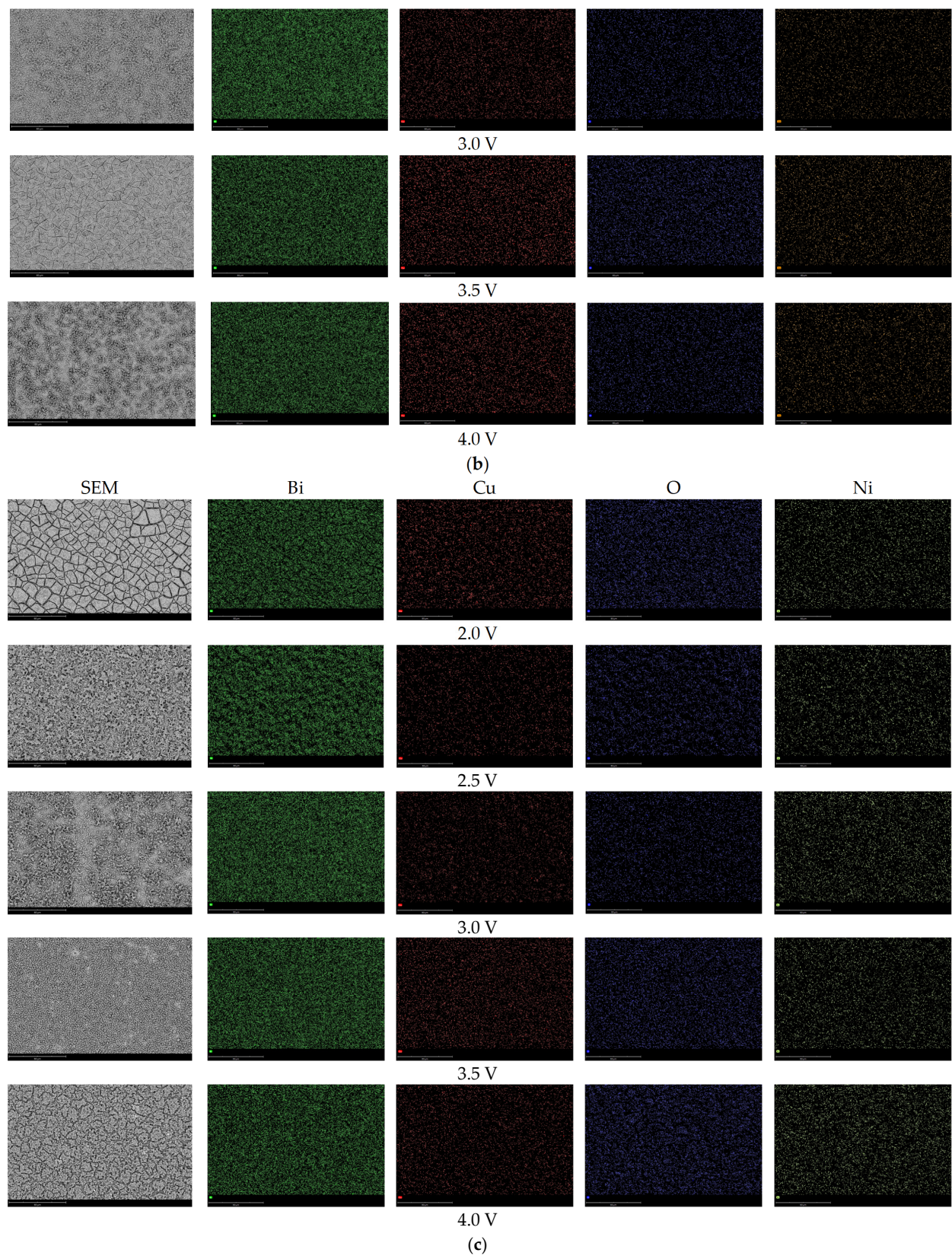


Figure 3. Cont.



**Figure 3.** Mapping results reflecting the isotropy of the distribution of elements in the composition of films synthesized under various conditions: (a) when using the electrolyte composition to obtain  $\text{CuBi/CuBi}_2\text{O}_4$  films; (b) when using the electrolyte composition to obtain  $\text{Cu(Co)Bi}_2\text{O}_4$  films; (c) when using the electrolyte composition to obtain  $\text{Cu(Ni)Bi}_2\text{O}_4$  films (under the diffraction patterns are line diagrams of cards from the PDF-2 (2016) database).

By analyzing changes in the elemental composition of the resulting CuBi/CuBi<sub>2</sub>O<sub>4</sub> films with changes in the applied potential difference, we can draw the following conclusions (see data in Figure 4) associated with the fact that the main changes in the elemental composition of films with an increase in the applied potential difference from 2.0 to 2.5 V occur due to an increase in the weight contribution of bismuth, the content of which increases from 6.6 at.% to 12.5 at.%. Moreover, such a change is in good agreement with the data on changes in the parameters of the crystal lattice presented in Table 1, as well as with the assumption made about the partial substitution of copper ions by bismuth ions during the formation of films. At the same time, the absence in the presented X-ray diffraction patterns of reflections characteristic of bismuth or other compounds of the substitutional solid solution type can be explained by low concentrations of bismuth in the structure of the films, as well as a well-structured crystal lattice of copper, the reflections of which are quite clearly visible in the diffraction patterns. It should also be noted that, when the applied potential difference increases to 3.0 V, a low oxygen content (no more than 2.5%) is observed in the structure of the resulting films, the presence of which can be explained by the structural formation of the films which, in the case of high potential differences, is accompanied by a rapid release of oxygen, which can penetrate into the films being formed, filling vacancies or interstices. In this case, also, the observed increase in the bismuth content in the films is in good agreement with the data on changes in structural parameters (data on the crystal lattice parameters are presented in Table 1 for the sample obtained at a potential difference of 3.0 V).

In the case of samples obtained at potential differences of 3.5 V, an increase in the content of bismuth (about 21 at.%) and oxygen (more than 5 at.%) is observed, which is consistent with X-ray diffraction data, according to which the diffraction pattern of the sample under study shows the appearance of low-intensity reflections at angular positions  $2\theta = 38.0, 40.5$  and  $46.0^\circ$ , characteristic of the tetragonal phase of CuBi<sub>2</sub>O<sub>4</sub> (PDF-01-071-5101); however, it is impossible to establish the weight contribution of it due to its low intensity. At the same time, for samples obtained at a potential difference of 4.0 V, the position of diffraction reflections is characteristic of the tetragonal phase of CuBi<sub>2</sub>O<sub>4</sub>, and when analyzing the elemental composition data, it was found that, at a given potential difference, a high content of oxygen and bismuth is observed in the structure of the films.

**Table 1.** Crystal lattice parameters of the films under study in the case of using different solutions–electrolytes.

Phase	When Using Solution–Electrolyte №1				
	Applied Potential Difference, V				
	2.0	2.5	3.0	3.5	4.0
Cu–Cubic (PDF-00-004-0836)	$a = 3.6086 \pm 0.0014 \text{ \AA}$ *	$a = 3.6114 \pm 0.0021 \text{ \AA}$	$a = 3.6148 \pm 0.0017 \text{ \AA}$	$a = 3.6163 \pm 0.0022 \text{ \AA}$	-
CuBi <sub>2</sub> O <sub>4</sub> –tetragonal (PDF-01-071-5101)	-	-	-	-	$a = 8.4607 \pm 0.0026 \text{ \AA}$ , $c = 5.8022 \pm 0.0025 \text{ \AA}$
Phase	When Using Solution–Electrolyte №2				
	Applied Potential Difference, V				
	2.0	2.5	3.0	3.5	4.0
CuBi <sub>2</sub> O <sub>4</sub> –tetragonal (PDF-01-071-5101)	$a = 8.4292 \pm 0.0023 \text{ \AA}$ , $c = 5.7072 \pm 0.0021 \text{ \AA}$	$a = 8.4359 \pm 0.0016 \text{ \AA}$ , $c = 5.6926 \pm 0.0023 \text{ \AA}$	$a = 8.4325 \pm 0.0015 \text{ \AA}$ , $c = 5.6758 \pm 0.0024 \text{ \AA}$	$a = 8.4258 \pm 0.0023 \text{ \AA}$ , $c = 5.6713 \pm 0.0022 \text{ \AA}$	$a = 8.4191 \pm 0.0017 \text{ \AA}$ , $c = 5.6668 \pm 0.0022 \text{ \AA}$
Phase	When Using Solution–Electrolyte №3				
	Applied Potential Difference, V				
	2.0	2.5	3.0	3.5	4.0
CuBi <sub>2</sub> O <sub>4</sub> –tetragonal (PDF-01-071-5101)	$a = 8.4738 \pm 0.0024 \text{ \AA}$ , $c = 5.8226 \pm 0.0022 \text{ \AA}$	$a = 8.4622 \pm 0.0026 \text{ \AA}$ , $c = 5.8124 \pm 0.0023 \text{ \AA}$	$a = 8.4572 \pm 0.0023 \text{ \AA}$ , $c = 5.8069 \pm 0.0015 \text{ \AA}$	$a = 8.4456 \pm 0.0024 \text{ \AA}$ , $c = 5.7965 \pm 0.0018 \text{ \AA}$	$a = 8.4373 \pm 0.0022 \text{ \AA}$ , $c = 5.7908 \pm 0.0014 \text{ \AA}$

\* parameter refinement was carried out by application of a method based on comparing the position of experimentally obtained diffraction patterns with the data of reference values taken from the PDF-2 (2016) database.

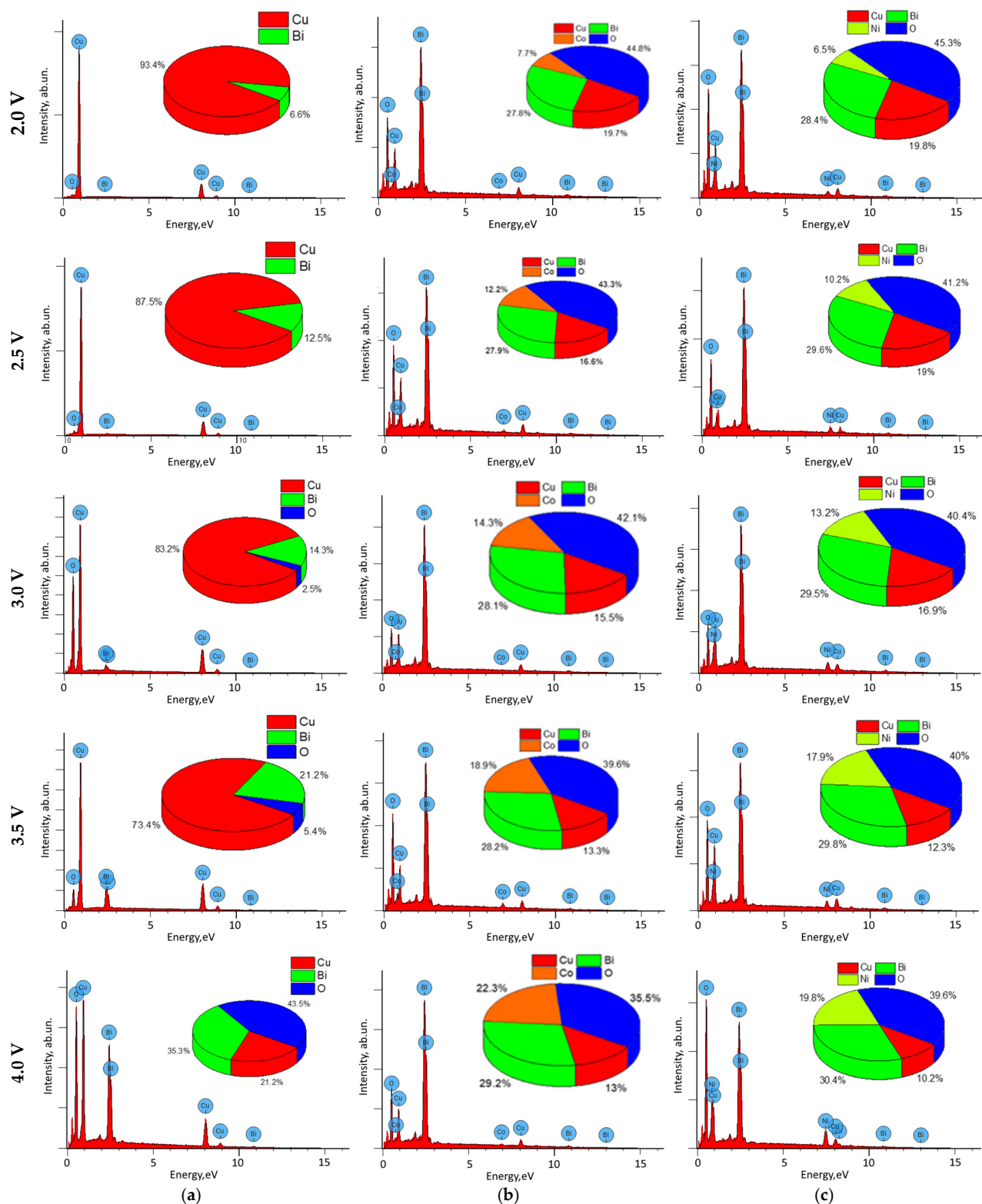


**Figure 4.** Results of energy dispersive analysis of films: (a) when using the electrolyte composition to obtain CuBi/CuBi<sub>2</sub>O<sub>4</sub> films; (b) when using the electrolyte composition to obtain Cu(Co)Bi<sub>2</sub>O<sub>4</sub> films; (c) when using the electrolyte composition to obtain Cu(Ni)Bi<sub>2</sub>O<sub>4</sub> films.

According to the obtained X-ray phase analysis data, it was established that, when the applied potential difference increases above 3.5 V, a phase transformation of the Cu(Bi) → CuBi<sub>2</sub>O<sub>4</sub> type is observed, which leads to the formation of films with a spinel type of crystal

structure and high density. It was established that, in the range of potential differences of 2.0–3.5 V, the dominant phase is the cubic phase of copper, the change in the parameters of the crystal lattice of which indicates the partial substitution of copper ions by bismuth ions while maintaining the cubic type of the crystal lattice. However, when the bismuth content in the films is more than 20 at.%, it leads to the initialization in the structure of the resulting films of phase transformations associated with the formation of the tetragonal  $\text{CuBi}_2\text{O}_4$  phase, which has a spinel type of crystal lattice.

Figure 2b demonstrates the results of X-ray diffraction of samples of  $\text{CuBi}/\text{CuBi}_2\text{O}_4$  films when a cobalt sulfate electrolyte was added to the solution, obtained by varying the applied potential difference. The obtained diffraction patterns indicate the polycrystalline structure of the synthesized films, and the observed changes depending on variations in synthesis conditions (changes in the applied potential difference) are characterized by changes in the degree of structural ordering, the change of which is associated with the processes of film formation during electrochemical synthesis.

According to the assessment of the phase composition for the studied  $\text{CuBi}/\text{CuBi}_2\text{O}_4$  films when cobalt sulfate electrolyte is added to the solution, it is established that the dominant phase is the tetragonal phase of  $\text{CuBi}_2\text{O}_4$ ; however, a significant difference from the observed similar phase for film samples obtained at an applied potential difference of 4.0 V when using electrolyte solution №1 is the broadening of parameter  $c$ , which indicates a deformation distortion of the crystal structure (see data in Table 1), which may be associated with the effects of replacing copper with cobalt. At the same time, a change in the synthesis conditions (i.e., a variation in the applied potential difference) in the case of adding cobalt sulfate to the electrolyte solution does not lead to phase change processes, and the structure of the resulting films in the entire studied range of the applied voltage difference is represented by the tetragonal  $\text{CuBi}_2\text{O}_4$  phase. This difference indicates that the addition of cobalt sulfate to the composition of the electrolyte solution leads to the acceleration of bismuth reduction processes at small differences in applied potentials, as well as the release of oxygen, which in turn leads to the formation of a tetragonal  $\text{CuBi}_2\text{O}_4$  phase with varying degrees of structural ordering.

It should also be noted that, when the applied potential difference changes, an increase in the degree of structural ordering is observed, which is expressed not only in a change in the shape of diffraction reflections (the reflections become more symmetrical), but also in a decrease in the parameters of the crystal lattice (see data in Table 1). From this, we can conclude that the addition of cobalt sulfate to the electrolyte solution results in the formation of highly ordered structures, and a change in synthesis conditions is accompanied by an increase in structural ordering.

Figure 4b reveals the assessment results of the change in the elemental composition of the synthesized films with varying applied potential difference, according to which we can conclude that, with an increase in the applied potential difference, copper is partially replaced by cobalt in the composition of the films, the content of which changes from 7.7 at.% at an applied potential difference of 2.0 V to 22.3 at.% at an applied potential difference of 4.0 V. At the same time, no change in the bismuth content in the composition of the films was observed when the synthesis conditions changed, which also indicates that the main substitution is associated with the displacement of copper and its substitution with cobalt. It is also worth noting that, when the applied potential difference changes, a slight decrease in oxygen is observed, the decrease of which may be due to structural ordering.

Figure 2c shows the results of X-ray diffraction of the studied samples of  $\text{CuBi}/\text{CuBi}_2\text{O}_4$  films when adding nickel sulfate electrolyte to the solution, obtained by changing the applied potential difference during the synthesis process. The general appearance of the obtained X-ray diffraction patterns indicates that a change in the applied potential difference leads to the formation of films with an almost X-ray amorphous structure (at small potential differences of 2.0–2.5 V), and in the case of high values of applied potential difference (3.5–4.0 V), well-structured films with a tetragonal type of crystal lattice, characteristic of the  $\text{CuBi}_2\text{O}_4$  phase. At the same time, as in the case of films obtained from an electrolyte

solution with the addition of cobalt sulfate (solution №2), the addition of nickel sulfate to the electrolyte solution also leads to structural ordering, which is most pronounced in changes in the structural parameters of the resulting films (see data presented in Table 1).

The data on changes in the elemental composition of the films presented in Figure 4c also indicate that the main substitution with a change in synthesis conditions (an increase in the applied potential difference) is associated with the displacement of copper and its substitution with nickel, the content of which also increases from 6.5 at.% at an applied potential difference of 2.0 V to 19.8 at.% at an applied potential difference of 4.0 V, which has a similar trend in the change in the elemental composition for films obtained from solution–electrolyte №2 (with the addition of cobalt sulfate to the electrolyte composition).

Analyzing the obtained changes in the elemental and phase composition of films obtained from solutions–electrolytes №2 and №3, we can conclude that an increase in the applied potential difference leads to the substitution of copper with cobalt or nickel, while new phase inclusions in the composition of the films have not been established.

Figure 5 presents the results of a comparative analysis of the degree of structural ordering (crystallinity degree)—a value that allows one to evaluate the perfection of the crystal structure of the resulting films, as well as the concentration of defective or disordered inclusions, a large number of which can lead to a decrease in the stability of films during their operation. The degree of crystallinity was assessed using a method based on approximating the obtained X-ray diffraction patterns with the required number of pseudo-Voigt functions in order to determine the ratio of the areas of diffraction reflections and the background area. By comparing these values, the degree of crystallinity was determined, i.e., structural ordering of the crystal structure of the obtained samples depending on the conditions of their preparation.

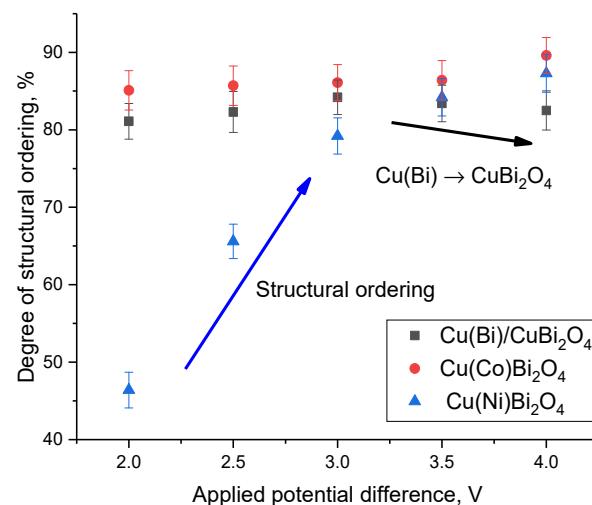
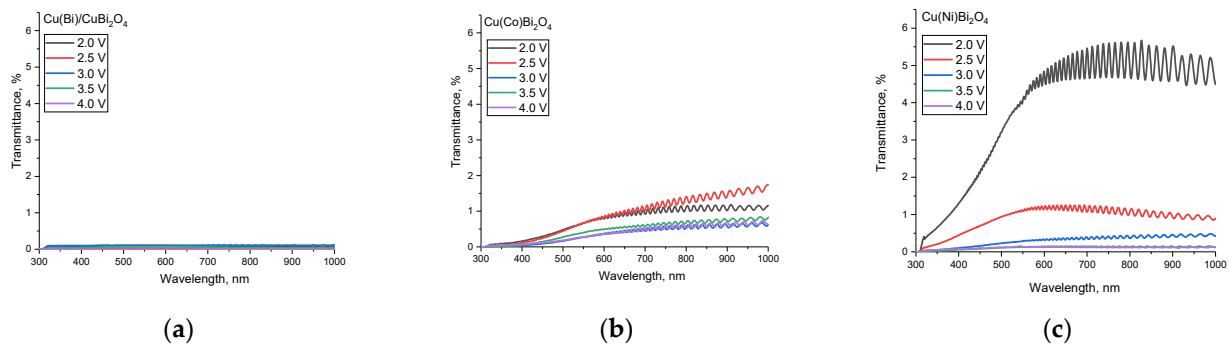


**Figure 5.** Results of the structural ordering degree of CuBi/CuBi<sub>2</sub>O<sub>4</sub> films depending on variations in synthesis conditions.

As can be seen from the presented data, the most pronounced changes in the degree of structural ordering are observed for CuBi/CuBi<sub>2</sub>O<sub>4</sub> films obtained from solution–electrolyte №3, for which, at small differences in applied potentials (2.0–2.5 V), the structural ordering degree has rather low values (less than 70%), which indicates a close to amorphous-like structure of the resulting films. Moreover, in the case of growth in the applied potential difference above 3.0 V, a more than twofold increase in the structural ordering degree for these films is observed in comparison with the results obtained with an applied potential difference of 2.0–2.5 V. The change in the structural ordering degree is close to linear for CuBi/CuBi<sub>2</sub>O<sub>4</sub> films obtained from solution–electrolyte №3, for which, according to X-ray diffraction data, structural ordering and compaction of the crystal lattice are observed (a decrease in its volume and parameters). In the case of using solution–electrolyte №1, there

is a slight decrease in the degree of structural ordering for samples obtained at applied potential differences of 3.5–4.0 V, which is due to phase transformation processes such as  $\text{Cu}(\text{Bi}) \rightarrow \text{CuBi}_2\text{O}_4$ .

Figure 6 reveals the results of determination of UV–Vis optical transmission spectra of synthesized films depending on the composition of the electrolyte used for synthesis. The general appearance of the obtained spectra is characterized by the presence of a fundamental absorption edge in the region of 300–350 nm, as well as a transmission spectrum in the visible and near-IR ranges. In the case of  $\text{CuBi}/\text{CuBi}_2\text{O}_4$  films, the optical spectra are straight with a very low transmission intensity (less than 1%), the value of which indicates the absence of transmission and complete absorption of light in the entire measured range. This nature of the optical spectra indicates the metallic nature of the films obtained, which causes the absence of light transmission. It is important to highlight that the formation of the  $\text{CuBi}_2\text{O}_4$  phase in the films at applied potential differences of 4.0 V leads to a slight increase in the transmission intensity, which may be due to phase changes in the films. In the case of addition of cobalt to the composition of the films, an elevation in transmission intensity is observed in the region above 500 nm, and in the case of the IR range, characteristic interference bands for the PET polymer film, which is the substrate for the synthesized films, are observed. A growth in cobalt content, meanwhile, results in a transmission intensity reduction, which is due to the metallization effect associated with the replacement of copper by cobalt, as well as changes in structural features and degree of crystallinity. For films obtained using an electrolyte with the addition of nickel sulfate, in the case where the films are of an X-ray amorphous nature, the transmittance in the visible and near-IR ranges is rather high, which indicates a direct influence of the degree of structural ordering on the optical properties of the synthesized films. In the case when  $\text{Cu}(\text{Ni})\text{Bi}_2\text{O}_4$  films become structurally ordered (at differences in applied potentials above 3.0 V), the optical transmittance decreases sharply.



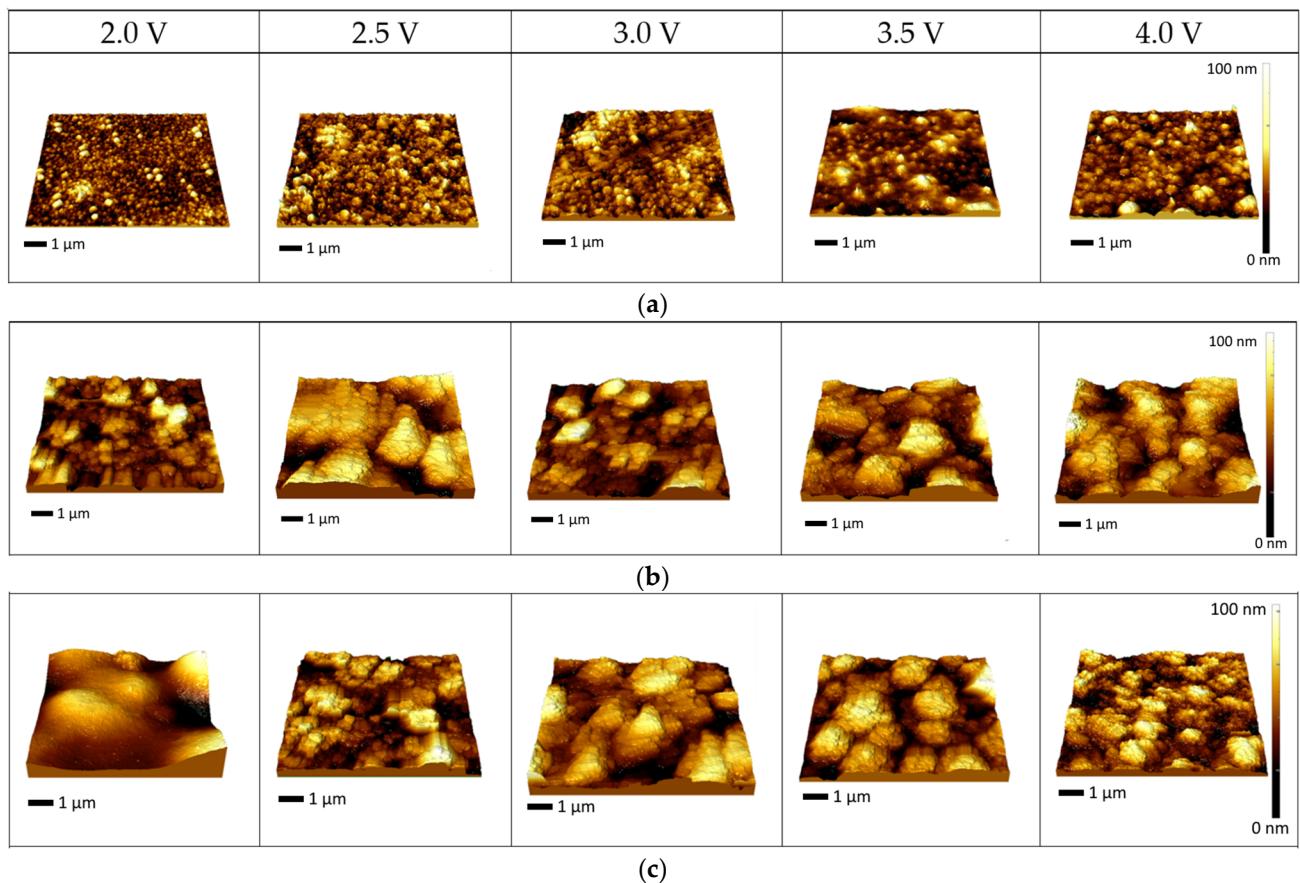
**Figure 6.** Measurement results of UV–Vis transmission spectra of synthesized films: (a) when using the electrolyte composition to obtain  $\text{CuBi}/\text{CuBi}_2\text{O}_4$  films; (b) when using the electrolyte composition to obtain  $\text{Cu}(\text{Co})\text{Bi}_2\text{O}_4$  films; (c) when using the electrolyte composition to obtain  $\text{Cu}(\text{Ni})\text{Bi}_2\text{O}_4$  films (data are shown on the same scale in order to compare the obtained spectra in terms of transmission intensity).

Figure 7a–c present the study results of the morphological features of the synthesized  $\text{CuBi}/\text{CuBi}_2\text{O}_4$  films depending on variations in synthesis conditions, as well as the type of solutions–electrolytes when nickel and cobalt sulfates are added to them. The data are presented in the form of 3D images of the surface of the samples, which reflect changes in both the shape of the grains (their sizes) and the packing density of the grains, expressed in the formation of agglomerates, the presence of which is characteristic of the formation of structures under various synthesis conditions.

The general appearance of the morphological features of  $\text{CuBi}/\text{CuBi}_2\text{O}_4$  films obtained from solution–electrolyte №1 indicates that a change in the applied potential differences leads to the enlargement of the grains from which the films are formed, and also that, under

all selected synthesis conditions, the surface of the resulting films is rather homogeneous (without large differences in profile heights and fairly low roughness values  $\sim 10\text{--}20$  nm). It follows from this that the use of the selected synthesis conditions is accompanied by the uniform growth of films, without any irregularities, and the deposition process itself is characterized by the formation of spherical or globular particles, the sizes of which vary depending on the synthesis conditions, and, as a consequence, the elemental composition of the resulting structures. The enlargement of grains during the synthesis process can be explained by the effects of accelerated nucleation, characteristic of electrochemical synthesis at large applied potential differences [34].

In the case of samples of the studied  $\text{CuBi}/\text{CuBi}_2\text{O}_4$  films obtained by the addition of cobalt sulfate electrolyte to a solution, changing the applied potential difference does not have a significant effect on the morphological features of the grains (no major changes in their sizes have been established); however, at large potential differences (above 3.0 V), the appearance of heterogeneities on the surface is observed, which indicates that the deposition of coatings is uneven (the difference is about 40–70 nm).



**Figure 7.** Three-dimensional images of the surface of the studied films: (a) when using the electrolyte composition to obtain  $\text{CuBi}/\text{CuBi}_2\text{O}_4$  films; (b) when using the electrolyte composition to obtain  $\text{Cu}(\text{Co})\text{Bi}_2\text{O}_4$  films; (c) when using the electrolyte composition to obtain  $\text{Cu}(\text{Ni})\text{Bi}_2\text{O}_4$  films.

During the electrochemical deposition of  $\text{CuBi}/\text{CuBi}_2\text{O}_4$  films obtained by adding a nickel sulfate electrolyte to a solution at an applied potential difference of 2.0 V, the formation of a fine-grained inhomogeneous structure is observed, which has good agreement with the results of X-ray diffraction, characterized by a structure close to X-ray amorphous in the resulting films, which can be explained by the formation of fine grains (the size of which is no more than 5 nm). A rise in the applied potential difference for these films leads to the formation of larger grains; however, as in the case of films obtained from solution-

electrolyte №2 (with the addition of cobalt sulfate), the resulting films are characterized by a fairly developed heterogeneous surface, presented in the form of large agglomerates of grains, the average size of which is about 1–2 microns in diameter.

Analyzing the data on changes in the morphological features of the resulting CuBi/CuBi<sub>2</sub>O<sub>4</sub> films from different compositions of solutions–electrolytes, we can conclude that the formation of the tetragonal CuBi<sub>2</sub>O<sub>4</sub> phase in the film structure leads to the enlargement of grains, and in the case of addition of cobalt or nickel sulfates to the composition of solutions–electrolytes, it leads to the formation of films with a fairly heterogeneous developed surface, which can be used as anti-friction coatings (resistant to wear).

### 3.2. Determination of the Influence of Variations in the Composition of Solutions–Electrolytes on the Strength Characteristics of CuBi/CuBi<sub>2</sub>O<sub>4</sub> Films

Determination of strength characteristics, as well as determination of the effect of addition of cobalt or nickel electrolyte to the solution, which is accompanied by a change in the structural features of the synthesized films, was carried out using the indentation method, the results of which are presented in Figure 8a. These measurements were carried out from different areas of the films under study in order to determine the uniformity of strength characteristics, as well as determine the measurement error and standard deviation.

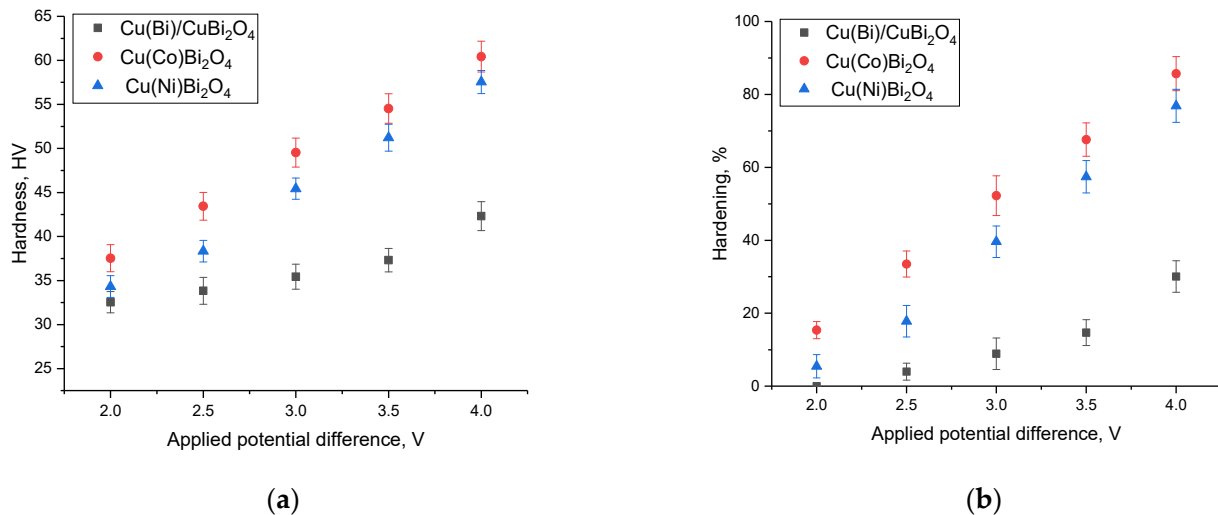


**Figure 8.** (a) Results of changes in the hardness of CuBi/CuBi<sub>2</sub>O<sub>4</sub> films obtained under different production conditions; (b) Results of strengthening of synthesized CuBi/CuBi<sub>2</sub>O<sub>4</sub> films obtained under different production conditions.

The presented dependences of changes in the hardness of CuBi/CuBi<sub>2</sub>O<sub>4</sub> films obtained under different production conditions can be divided into two types: the first type of changes is associated with the influence of variations in solutions–electrolytes used for film synthesis; the second type with changes in the applied potential difference, which, according to the presented X-ray diffraction data, is accompanied by a change in the degree of structural ordering (when using solutions–electrolytes №2 and №3), as well as phase transformations such as Cu(Bi) → CuBi<sub>2</sub>O<sub>4</sub> (when using solution–electrolyte №1 at potential differences above 3.5 V).

In the case of changes in the hardness values of film samples of the first type, we can conclude that the addition of cobalt or nickel sulfate to the electrolyte solutions leads to an increase in hardness values, which are most pronounced at high potential differences. This increase in hardness can be explained by phase changes in the films, which consist in the fact that, when using solutions–electrolytes №2 and №3, the phase composition of the films is presented in the form of a tetragonal CuBi<sub>2</sub>O<sub>4</sub> phase, with partial substitution of copper by cobalt or nickel, while the samples obtained from solution–electrolyte №1 at

applied potential differences from 2.0 to 3.0 V are represented by the cubic Cu phase, in which some of the atomic positions are occupied by bismuth.

The second type of changes in the hardness values of the film samples under study is associated with the influence of the degree of structural ordering, as well as changes in the elemental composition of the resulting films (an increase in the bismuth content in the case of using electrolyte solution №1 and partial substitution of copper with cobalt or nickel when using electrolyte solutions №2 and №3, respectively). In this case, an increase in these elements in the composition of films leads to a change in hardness (increase in hardness), which is most pronounced at large differences in applied potentials. The change in hardness with a change in the elemental and phase composition of the films is associated with structural changes, which are characterized by the effects of structural ordering (see data in Table 1).

Based on the obtained data on changes in hardness values, hardening factors were calculated, which characterize the effect of changes in strength parameters depending on changes in the degree of structural ordering and phase composition of CuBi/CuBi<sub>2</sub>O<sub>4</sub> films obtained under different production conditions. The hardening factor was calculated for CuBi/CuBi<sub>2</sub>O<sub>4</sub> films obtained under different synthesis conditions (in the case of variation in the applied potential difference) by comparative analysis of changes in the hardness values of the samples with the hardness data obtained for samples of CuBi/CuBi<sub>2</sub>O<sub>4</sub> films synthesized from solution–electrolyte №1 at a potential difference of 2.0 V. The results of the strength characteristics assessment are presented in Figure 8b.

The general appearance of the presented changes in the results of strengthening indicates that the greatest influence on the increase in strength characteristics is exerted by the effect of partial substitution of copper with cobalt or nickel, as well as an increase in their concentration in the films, which leads to more than 1.5-fold strengthening of the films. In the case of films obtained from a solution–electrolyte №1, the change in hardness (i.e., hardening) is most pronounced during phase transformations of the Cu(Bi) → CuBi<sub>2</sub>O<sub>4</sub> type, which lead to film strengthening by more than 20–25%, in comparison with films obtained at lower potential differences (below 3.0 V).

Figure 9 shows the results of a comparative analysis of the factors of structural ordering and film strengthening (hardness changes) depending on the type of films obtained. As can be seen from the presented dependence, the most pronounced effect of structural ordering on strengthening is manifested for CuBi/CuBi<sub>2</sub>O<sub>4</sub> films obtained from solution–electrolyte №3 (with the addition of nickel sulfate), the use of which, at potential differences equal to 2.0 and 2.5 V, leads to the formation of films with an almost X-ray amorphous structure, the ordering of which leads to a sharp change in strength characteristics. In the case of CuBi/CuBi<sub>2</sub>O<sub>4</sub> films obtained from solution–electrolyte №1, the main contribution to strengthening is made by phase transformation processes, which manifest themselves at applied potential differences above 3.0 V (in this case, the structural ordering degree for these films decreases due to phase transformations accompanied by deformation distortion of the crystal lattice due to rearrangement of the crystal structure and the formation of the tetragonal CuBi<sub>2</sub>O<sub>4</sub> phase).

One of the key factors characterizing the wear resistance of materials is their resistance to long-term mechanical stress due to friction or pressure. To assess wear resistance, as a rule, tribological methods are used, which make it possible to determine such quantities as the coefficient of dry friction, wear rate or mass loss of samples during long-term life tests.

Figure 10 shows the results of tribological tests of the studied CuBi/CuBi<sub>2</sub>O<sub>4</sub> films carried out with sequential exposure of the indenter to the surface of film samples. Based on the tribological test data, the dry friction coefficient was calculated, the value of which was measured after each 1000 consecutive tests. The general appearance of the presented dependences of changes in the dry friction coefficient when changing the type of solution–electrolyte for producing CuBi/CuBi<sub>2</sub>O<sub>4</sub> films can be characterized as follows. The use of solutions–electrolytes №2 and №3 leads to a slight increase in the coefficient of dry friction of films in the initial state from 0.24 to 0.25 in comparison with the value of the coefficient

of dry friction for CuBi/CuBi<sub>2</sub>O<sub>4</sub> films obtained from solution–electrolyte №1 equal to 0.17. This increase can be explained by effects associated with changes in the morphological features of the resulting films when using solutions–electrolytes №2 and №3, for which, according to the results of atomic force microscopy presented in Figure 4a–c, an increase in the surface roughness of the films and an enlargement of their sizes are observed. Moreover, for all three types of films, regardless of the applied potential differences, no significant differences in the initial value of the dry friction coefficient were observed.

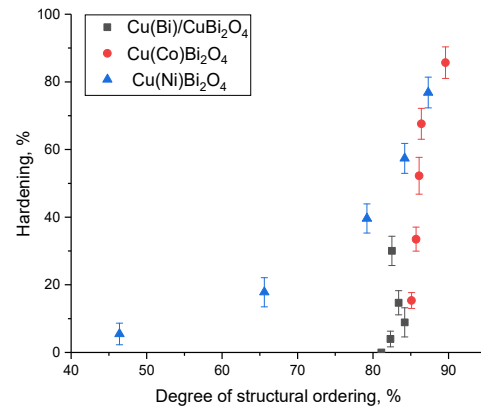


Figure 9. Results of a comparative analysis of factors of structural ordering and strengthening.

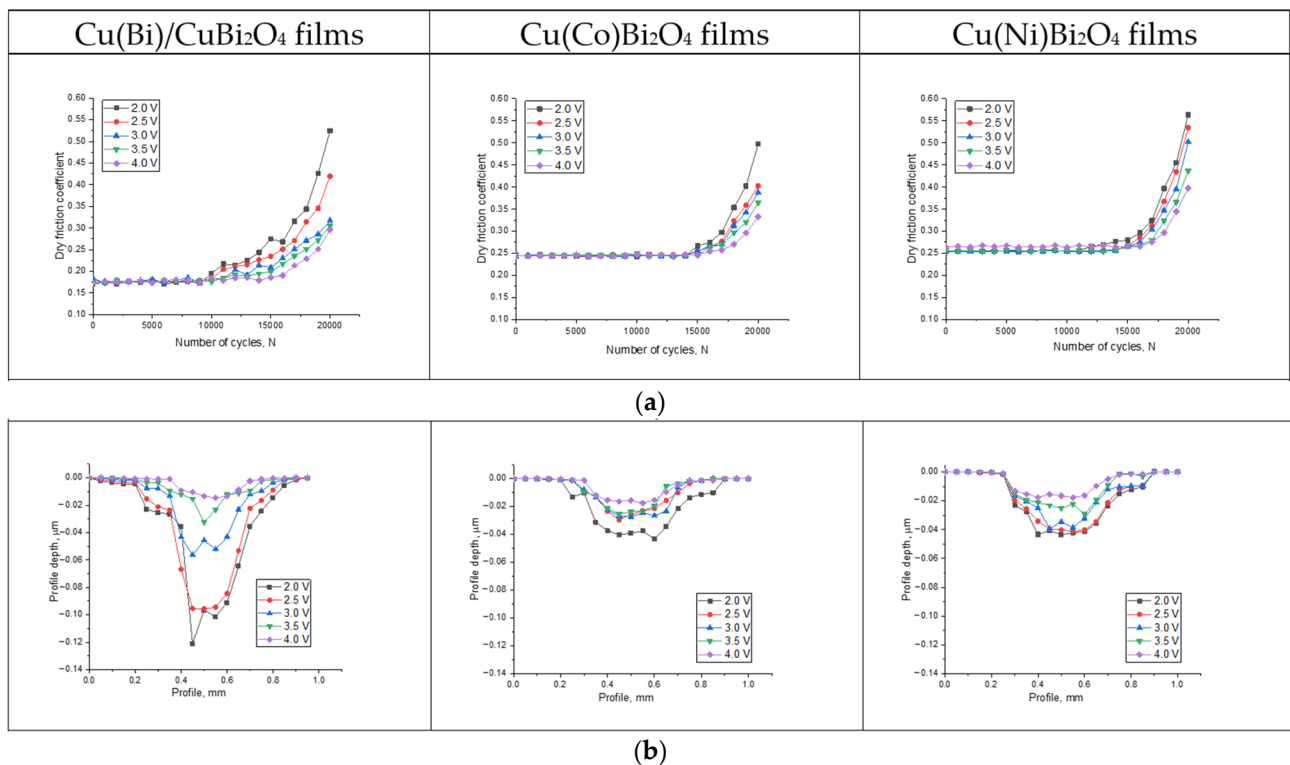
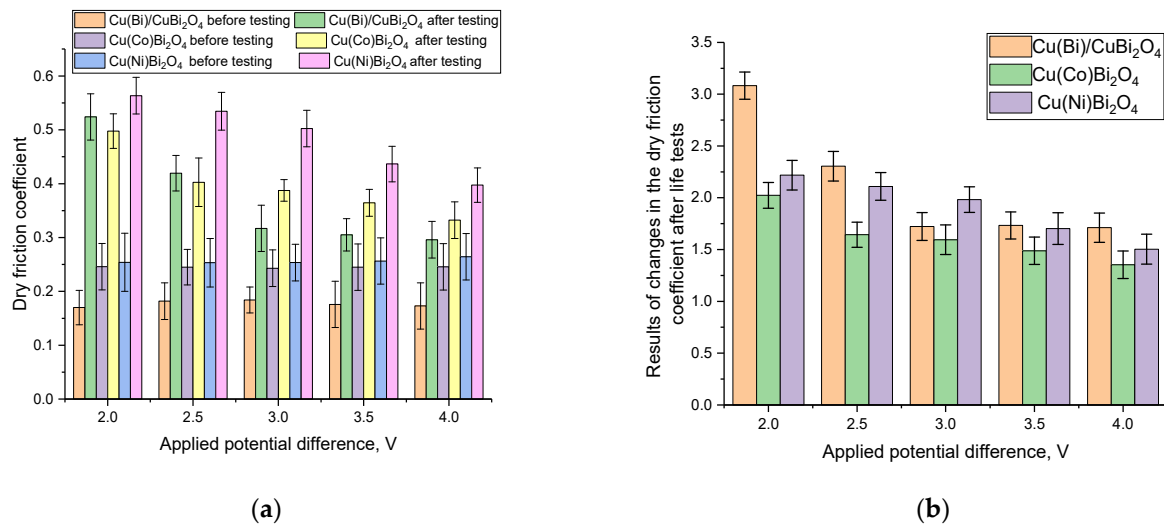


Figure 10. (a) Results of measurement of dry friction coefficient depending on the number of test cycles; (b) Results of evaluation of wear profile of film samples depending on their production conditions.

During long-term tests, a change in the dry friction coefficient (its increase) indicates surface degradation and wear, which leads to the creation of additional obstacles for the moving indenter and increases friction.

As a rule, wear-resistant coatings are able to withstand a fairly large number of test cycles (about 10,000–15,000), which characterizes their resistance to external influences. In the case of CuBi/CuBi<sub>2</sub>O<sub>4</sub> film samples obtained using electrolyte solution №1, the main changes in the dry friction coefficient are observed after 10,000 cycles, while the most pronounced changes occur after 15,000 cycles and consist of a sharp deterioration in the coefficient (see data in Figure 11a). At the same time, the most pronounced changes are observed for films obtained at potential differences of 2.0–3.0 V, in which the cubic phase of copper dominates, which has a fairly low resistance to degradation during wear resistance tests. In turn, phase transformations of the type Cu(Bi) → CuBi<sub>2</sub>O<sub>4</sub>, which occur at applied potential differences above 3.5 V (in the case of using electrolyte solution №1), lead to a decrease in the degradation of the dry friction coefficient in comparison with the initial values, which indicates an increase in the resistance of films to long-term mechanical influences (friction) in the case wherein the phase composition of the films is represented by the tetragonal CuBi<sub>2</sub>O<sub>4</sub> phase, which has higher hardness values than copper coatings with partial substitution of copper by bismuth.



**Figure 11.** (a) Results of a comparative analysis of changes in the value of the dry friction coefficient before and after tribological tests; (b) Results of evaluation of changes in the dry friction coefficient after the tribological life tests compared to the initial value (this change reflects the dry friction coefficient degradation degree during the tests).

In the case of films obtained using solutions–electrolytes №2 and №3, changes in the dry friction coefficient occur after 15,000 consecutive tests, and the degradation of the coefficient is about 1.5–2.0 times, while the degradation of the dry friction coefficient for films obtained using solution–electrolyte №1 is more than 2.5–3.0 times in comparison with the initial data (see data in Figure 11a,b).

Thus, analyzing the obtained results of changes in the value of the dry friction coefficient, we can conclude that the formation of films with a phase composition presented in the form of a tetragonal CuBi<sub>2</sub>O<sub>4</sub> phase leads to an increase in wear resistance and maintaining resistance to degradation during friction over a long number of cyclic tests, and in the case of partial substitution of copper with cobalt or nickel, an increase in wear resistance and a decrease in degradation of the film surface during tribological tests are observed.

Figure 10b shows the results of assessing the wear profile of the studied CuBi/CuBi<sub>2</sub>O<sub>4</sub> films depending on the production conditions, as well as the electrolyte solutions used (with the addition of cobalt or nickel sulfates). These profiles were obtained after conducting tribological tests for resistance to friction, and the profiles themselves reflect changes in the resistance of films to mechanical degradation caused by external mechanical influences (in this case, friction).

According to the data obtained, it is clear that the greatest changes associated with the degradation of the film surface are observed for copper films (samples obtained using solution–electrolyte №1 at potential differences from 2.0 to 3.0 V). At the same time, the assessment of wear profiles (i.e., depth and width of the profile) for samples obtained using solution–electrolyte №1 indicates that an increase in the concentration of bismuth in the composition of the films leads to an increase in wear resistance, which also manifests itself for samples obtained from solutions–electrolytes №2 and №3 when their elemental composition changes (when copper is replaced by cobalt or nickel). Moreover, in the case of films obtained from solutions–electrolytes №2 and №3, the wear profiles have a significantly shallower depth, in comparison with similar profile data obtained for films synthesized using solution–electrolyte №1, which indicates their high resistance to external influences, in particular to the loss of sample mass during prolonged friction.

Based on the obtained data on changes in the dry friction coefficient, as well as wear profiles, the wear rate was calculated during tribological tests of the surface of films obtained from various solutions–electrolytes and when changing synthesis conditions (variations in the applied potential difference). The evaluation results are presented in Figure 12 in the form of a comparison chart.

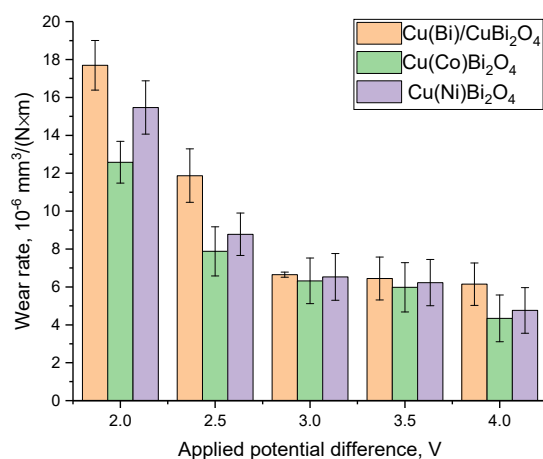


**Figure 12.** Results of film wear rate assessment during tribological tests.

According to the data obtained, the films obtained at an applied potential difference of 2.0 for all three types of solutions–electrolytes have the highest degradation rate (surface wear rate during life-long tribological tests), which is due to structural (in the case of films obtained from a solution–electrolyte №1, a high concentration of copper) or morphological features (in the case of films obtained from solution–electrolyte №3, an amorphous-like structure consisting of small grains), which leads to the accelerated degradation of films. Moreover, in the case when the concentration of cobalt or nickel in the film composition increases (when using solutions–electrolytes №2 and №3), as well as bismuth (when using a solution–electrolyte №1), a more than 2.0–2.5-fold decrease in the surface wear rate is observed, which is expressed in lower changes in the dry friction coefficient, as well as smaller wear profiles.

Thus, summing up the results of the measurements of the strength and tribological characteristics of the films under study, we can conclude that the substitution of copper with cobalt or nickel that occurs in the structure of the films leads to the possibility of obtaining high-strength wear-resistant films that are highly resistant to long-term mechanical influences.

Resistance to mechanical influences, in particular mechanical pressure, shock and friction, is one of the important parameters when using protective materials in real conditions. Thus, good wear resistance indicators allow for the use of these protective coatings during mechanical friction in the case when moving parts are used that can come into contact with

each other during operation. In this case, high resistance to wear due to friction makes it possible to eliminate the factors of destruction of coatings during prolonged mechanical action, as well as to avoid the effects associated with a decrease in shielding efficiency in the case of partial or complete separation of coatings from the surface. Comparing the hardness values of the synthesized coatings with similar nitride (TiN) coatings obtained by magnetron sputtering [35,36] or by vapor deposition [37], they are approximately 1.5–2.0 times lower than the hardness of TiN coatings [36], and 7–10 times lower than coatings obtained by vapor deposition [37]. In comparison with carbide coatings [38,39], the hardness values of  $\text{CuBi}/\text{CuBi}_2\text{O}_4$ ,  $\text{Cu}(\text{Co})\text{Bi}_2\text{O}_4$  and  $\text{Cu}(\text{Ni})\text{Bi}_2\text{O}_4$  films are also approximately 5–6 times lower. However, comparing wear resistance indicators determined from changes in the dry friction coefficient, we can conclude that the synthesized films under consideration have comparable wear resistance indicators to carbide and nitride coatings during long-term wear tests. This difference is due to the peculiarities of the coating production methods, as well as differences in the scope of application. As a rule, nitride coatings are used to protect against corrosion and degradation of steel structures, but do not have high shielding characteristics.

### 3.3. Determination of Gamma Ray Shielding Efficiency Using Different Films

To determine the shielding efficiency of gamma radiation with energies of 0.13, 0.66 and 1.23 MeV generated by  $\text{Co}^{57}$ ,  $\text{Cs}^{137}$ ,  $\text{Na}^{22}$  sources, respectively, five samples of  $\text{CuBi}/\text{CuBi}_2\text{O}_4$  films obtained under different conditions were selected: Cu films with a low bismuth content, obtained from electrolyte solution №1 at an applied potential difference of 2.0 V, Cu(Bi) films with a bismuth content of about 20 at.%, obtained from an electrolyte solution at an applied potential difference of 3.5 V,  $\text{CuBi}_2\text{O}_4$  films obtained from electrolyte solution №1 at a potential difference of 4.0 V,  $\text{Cu}(\text{Co})\text{Bi}_2\text{O}_4$  and  $\text{Cu}(\text{Ni})\text{Bi}_2\text{O}_4$  films obtained at an applied potential difference of 4.0 V from electrolyte solutions №2 and №3, respectively. Shielding experiments were carried out according to a standard scheme; the efficiency was assessed using the calculation formulas used in [40–42], which make it possible to obtain the values of the shielding characteristics of films, which were compared with the calculated values performed using the XCOM code, the simulation results of which are presented in Figure 13.

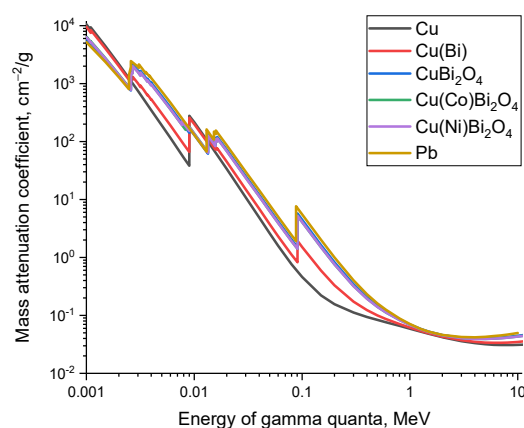


**Figure 13.** Calculation results of the mass attenuation coefficient obtained using the XCOM program code (data on changes in the mass attenuation coefficient for lead are also given as an example).

The general appearance of the presented dependences of the change in the mass attenuation coefficient indicates the presence of local absorption maxima and minima, characteristic of the structural features of the films, as well as their electronic structure. At the same time, the analysis of the obtained dependences showed high values of the absorbing (shielding) ability of the selected objects of study in the region of low energies of gamma quanta (less than 0.1 MeV), characteristic of the processes of interaction of gamma quanta through the mechanisms of the photoelectric effect. At the same time, no significant

differences are observed in the energy region of more than 1 MeV, since in this region the dominant role is played by the processes of formation of electron–positron pairs, the formation of which is accompanied by the effects of the formation of secondary radiation. Also shown in Figure 10 is the dependence of the mass attenuation coefficient for lead, which has the maximum shielding efficiency for gamma radiation among all currently known protective shielding materials. As can be seen from a comparative analysis of the dependences of the mass attenuation coefficient for the films under study with data for lead, the most pronounced changes are observed for samples in the energy range of gamma radiation up to 1 MeV, where the processes of the photoelectric effect and the Compton effect dominate, while in the region of high-energy gamma quanta (with energy of more than 1.0 MeV), the dependences have almost the same range of values.

The assessment results of the shielding characteristics (mass and linear attenuation coefficient, half-attenuation thickness and mean free path) are presented in Table 2. The general appearance of the presented dependences of the shielding characteristics indicates the positive influence of phase transformations such as  $\text{Cu}(\text{Bi}) \rightarrow \text{CuBi}_2\text{O}_4$ , as well as the substitution of copper with cobalt and nickel in the composition of  $\text{Cu}(\text{Co})\text{Bi}_2\text{O}_4$  and  $\text{Cu}(\text{Ni})\text{Bi}_2\text{O}_4$  films, which leads to an increase in the efficiency of shielding characteristics by more than 3.0–4.0 times when shielding gamma quanta with energies of 0.13 MeV in comparison with Cu films, which have minimal gamma-ray shielding efficiency indicators. In the case of shielding gamma rays with energies of 0.66 and 1.23 MeV, the difference in the efficiency of shielding characteristics in comparison with Cu films is about 1.5–2.0 times, which is due to differences in the mechanisms of interaction of gamma quanta with higher energies, which are accompanied by the formation of secondary radiation.

**Table 2.** Data on the shielding characteristics of the thin film samples under study.

Sample Type	Shielding Parameter for Gamma Rays with an Energy of 0.13 MeV ( $\text{Co}^{57}$ )			
	MAC, $\text{cm}^2/\text{g}$	LAC, $\text{cm}^{-1}$	$\Delta_{1/2}$ , $\text{cm}^{-1}$	MFP, cm
Cu *	0.39	3.47	0.20	0.29
Cu(Bi)	1.42	11.84	0.06	0.08
$\text{CuBi}_2\text{O}_4$	1.59	13.63	0.05	0.07
$\text{Cu}(\text{Co})\text{Bi}_2\text{O}_4$	1.85	16.01	0.04	0.06
$\text{Cu}(\text{Ni})\text{Bi}_2\text{O}_4$	1.73	14.93	0.05	0.07
Sample Type	Shielding Parameter for Gamma Rays with an Energy of 0.66 MeV ( $\text{Cs}^{137}$ )			
	MAC, $\text{cm}^2/\text{g}$	LAC, $\text{cm}^{-1}$	$\Delta_{1/2}$ , $\text{cm}^{-1}$	MFP, cm
Cu	0.067	0.60	1.16	1.68
Cu(Bi)	0.075	0.63	1.11	1.61
$\text{CuBi}_2\text{O}_4$	0.105	0.90	0.77	1.11
$\text{Cu}(\text{Co})\text{Bi}_2\text{O}_4$	0.113	0.98	0.71	1.02
$\text{Cu}(\text{Ni})\text{Bi}_2\text{O}_4$	0.111	0.96	0.72	1.04
Sample Type	Shielding Parameter for Gamma Rays with an Energy of 1.23 MeV ( $\text{Na}^{22}$ )			
	MAC, $\text{cm}^2/\text{g}$	LAC, $\text{cm}^{-1}$	$\Delta_{1/2}$ , $\text{cm}^{-1}$	MFP, cm
Cu	0.039	0.35	2.01	2.88
Cu(Bi)	0.048	0.40	1.73	2.51
$\text{CuBi}_2\text{O}_4$	0.052	0.45	1.56	2.24
$\text{Cu}(\text{Co})\text{Bi}_2\text{O}_4$	0.058	0.50	1.38	1.99
$\text{Cu}(\text{Ni})\text{Bi}_2\text{O}_4$	0.054	0.47	1.49	2.15

\* Values are given to reflect the low efficiency of using Cu films as protective shielding materials.

The data on alterations in shielding characteristics presented in Table 2 demonstrate that the addition of cobalt to films leads to an increase in MAC efficiency by 15–16% in comparison with  $\text{CuBi}_2\text{O}_4$  films and about 30% in comparison with  $\text{Cu}(\text{Bi})$  films. In the case of adding nickel to the film composition, the efficiency of MAS increases by 8–10% when compared with  $\text{CuBi}_2\text{O}_4$  films and by about 21–22% when compared with  $\text{Cu}(\text{Bi})$  films. Thus, it can be concluded that the addition of cobalt and nickel to the composition, which makes it possible to obtain films with the structure of  $\text{Cu}(\text{Co})\text{Bi}_2\text{O}_4$  and  $\text{Cu}(\text{Ni})\text{Bi}_2\text{O}_4$ , results in an elevation in the shielding efficiency of the order of 10–20%. Moreover, these films have higher levels of mechanical strength and wear resistance to external influences, which together allows them to be used as protective coatings exposed to external mechanical influences, friction during use, etc.

Figure 14a presents the results of a comparative analysis of the experimentally determined values of the mass attenuation coefficient of the films selected as objects of study with the simulation results performed using the XCOM code. According to the data presented, there is good agreement between the experimental and calculated values of the mass attenuation coefficient (the difference is no more than 10%), which indicates that the obtained experimental values of the shielding characteristics reliably reflect the effectiveness of the synthesized films.

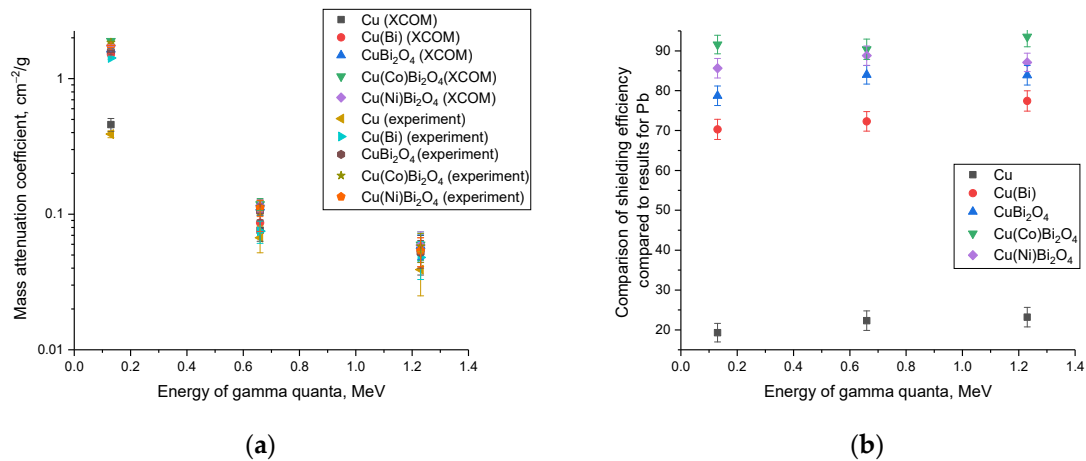


**Figure 14.** (a) Results of a comparative analysis of the mass attenuation coefficient obtained experimentally and using the modeling method in the XCOM code; (b) Results of evaluation of the shielding efficiency of  $\text{CuBi}/\text{CuBi}_2\text{O}_4$  films in comparison with the mass attenuation coefficient of Pb films obtained on the basis of calculated data using the XCOM program code.

Figure 14b presents the results of the shielding efficiency (mass attenuation coefficient) of the films under study for all three types of gamma ray energy in comparison with the value of the mass attenuation coefficient of lead obtained from the simulation results using the XCOM code. As can be seen from the presented data, the synthesized  $\text{CuBi}_2\text{O}_4$  films obtained from solution–electrolyte №1 at a potential difference of 4.0 V,  $\text{Cu}(\text{Co})\text{Bi}_2\text{O}_4$  and  $\text{Cu}(\text{Ni})\text{Bi}_2\text{O}_4$  films, have a shielding efficiency of the order of 0.8–0.9 of the value of the shielding characteristics of lead; however, the density of the films is significantly lesser than the density of lead, and as a result, the use of these films as shielding protective materials will reduce the weight and overall dimensions by reducing the weight of the shields, without losing shielding efficiency (the reduction in shielding efficiency when using these films will be no more than 10–20%). It is also worth to note that the use of the effect of replacing copper with cobalt or nickel in the composition of the tetragonal phase of  $\text{CuBi}_2\text{O}_4$  leads to an increase in the shielding efficiency by 5–10% in comparison with samples of  $\text{CuBi}_2\text{O}_4$  films without substitution, which also indicates the positive effect of using dopants to modify the resulting films.

#### 4. Conclusions

In the course of the studies carried out using the X-ray diffraction method, results were obtained on changes in the phase composition of films with variations in synthesis conditions (differences in applied potentials) and changes in the compositions of solutions–electrolytes (with the addition of cobalt and nickel sulfates). In the case of using solution–electrolyte №1 (without any additives), a change in the applied potential difference leads to the initialization of phase transformation processes such as  $\text{Cu}(\text{Bi}) \rightarrow \text{CuBi}_2\text{O}_4$ , which occur when the applied potential differences are above 3.0 V, as well as when the bismuth content in the films is about 20 at.% and higher. In this case, in the case of small applied potential differences (below 3.0 V), the dominance of the cubic copper phase was observed in the structure of the films, the change in the structural parameters for which indicates the processes of partial substitution of copper with bismuth (substitution or interstitial phase).

When using solutions–electrolytes №2 and №3 (addition of cobalt sulfate and nickel sulfate, respectively), the dominant phase in the film structure is the tetragonal  $\text{CuBi}_2\text{O}_4$  phase, for which a change in the applied potential difference during film deposition leads to an increase in structural ordering, as well as a decrease in the crystal lattice parameters, indicating film densification. At the same time, analysis of these changes in the elemental composition of films when using solutions–electrolytes №2 and №3 indicates that the main changes are associated with the substitution of copper with cobalt or nickel (depending on the type of electrolyte solution used), the concentrations of which grow with an increase in the applied potential differences.

The results of studies of the strength and tribological characteristics of the synthesized films, depending on the conditions for their production, showed the following. It has been experimentally established that the addition of cobalt or nickel sulfates to the composition of solutions–electrolytes №2 and №3 leads to an increase in the strength of the resulting films from 20 to 80%, depending on the production conditions (with variations in the difference in applied potentials). In the course of determining the tribological characteristics, it was found that, when replacing copper with cobalt or nickel, depending on the type of solution–electrolyte used, as well as synthesis conditions (in the case of varying the difference in applied potentials), an increase in resistance to wear is observed, as well as a decrease in the wear profile, which indicates an increase in wear resistance and degradation to external mechanical influences. At the same time, alterations in the morphological features of  $\text{CuBi}/\text{CuBi}_2\text{O}_4$  films depending on variations in synthesis conditions (changes in the electrolyte solution or the difference in applied potentials) do not lead to significant changes in the dry friction coefficient.

When determining the shielding efficiency of gamma radiation, it was found that replacing copper with cobalt or nickel in the composition of  $\text{CuBi}_2\text{O}_4$  films leads to an increase in the shielding efficiency of low-energy gamma radiation by 3.0–4.0 times in comparison with copper films, and 1.5–2.0 times for high-energy gamma quanta. The efficiency decrease in this case is due to differences in the mechanisms of interaction of gamma quanta, as well as the occurrence of secondary radiation as a result of the formation of electron–positron pairs and the Compton effect. It was found that the use of the effect of substitution of copper with cobalt or nickel in the composition of the tetragonal phase of  $\text{CuBi}_2\text{O}_4$  results in an elevation in the shielding efficiency by 5–10% in comparison with samples of  $\text{CuBi}_2\text{O}_4$  films without substitution, which also indicates the positive effect of using dopants to modify the resulting films.

**Author Contributions:** Conceptualization, M.T.I., A.L.K., D.I.S. and D.B.K.; methodology, M.T.I., A.L.K., D.I.S. and D.B.K.; formal analysis, M.T.I., A.L.K., D.I.S. and D.B.K.; investigation, M.T.I., A.L.K., D.I.S. and D.B.K.; resources, M.T.I., A.L.K., D.I.S. and D.B.K.; writing—original draft preparation, review, and editing, M.T.I., A.L.K., D.I.S. and D.B.K.; visualization, M.T.I., A.L.K., D.I.S. and D.B.K.; supervision, D.B.K. All authors have read and agreed to the published version of the manuscript.

**Funding:** This study was funded by the Science Committee of the Ministry of Science and Higher Education of the Republic of Kazakhstan (No. AP14871152).

**Data Availability Statement:** The original contributions presented in the study are included in the article, further inquiries can be directed to the corresponding author.

**Conflicts of Interest:** The authors declare no conflicts of interest.

## References

1. National Research Council; Division on Earth and Life Studies; Nuclear and Radiation Studies Board; Committee on Radiation Source Use and Replacement. *Radiation Source Use and Replacement: Abbreviated Version*; National Academies Press: Washington, DC, USA, 2008; pp. 1–100.
2. Kottou, S.; Nikolopoulos, D.; Vogianis, E.; Koulougliotis, D.; Petraki, E.; Yannakopoulos, P.H. How safe is the environmental electromagnetic radiation. *J. Phys. Chem. Biophys.* **2014**, *4*, 1000146. [\[CrossRef\]](#)
3. Panagopoulos, D.J.; Margaritis, L.H. 2. Theoretical Considerations for the Biological Effects of Electromagnetic Fields. In *Biological Effects of Electromagnetic Fields: Mechanisms, Modeling, Biological Effects, Therapeutic Effects, International Standards, Exposure Criteria*; Springer: Berlin/Heidelberg, Germany, 2013; p. 2.
4. Classic, K.; Le Guen, B.; Kase, K.; Vetter, R. Safety and radiation protection culture. In *Radiological Safety and Quality: Paradigms in Leadership and Innovation*; Springer: Dordrecht, The Netherlands, 2014; pp. 263–277.
5. Gutierrez, J.M.; Emery, R.J. A 30-year radiation safety prospectus describing organizational drivers, program activities, and outcomes. *Health Phys.* **2022**, *122*, 352–359. [\[CrossRef\]](#) [\[PubMed\]](#)
6. Moore, Q.T. Validity and reliability of a radiation safety culture survey instrument for radiologic technologists. *Radiol. Technol.* **2021**, *92*, 547–560. [\[PubMed\]](#)
7. Morris, V. A quality educational program can significantly improve radiation safety. *Health Phys.* **2003**, *84*, S71–S73. [\[CrossRef\]](#) [\[PubMed\]](#)
8. Mirzayev, M.N.; Popov, E.; Demir, E.; Abdurakhimov, B.A.; Mirzayeva, D.M.; Sukratov, V.A.; Mutali, A.K.; Tjep, V.N.; Biira, S.; Tashmetov, M.Y.; et al. Thermophysical behavior of boron nitride and boron trioxide ceramics compounds with high energy electron fluence and swift heavy ion irradiated. *J. Alloys Compd.* **2020**, *834*, 155119. [\[CrossRef\]](#)
9. Abdelbagi, H.A.; Skuratov, V.A.; Motloun, S.V.; Njoroge, E.G.; Mlambo, M.; Hlatshwayo, T.T.; Malherbe, J.B. Effect of swift heavy ions irradiation on the migration behavior of strontium implanted into polycrystalline SiC. *Nucl. Instrum. Methods Phys. Res. Sect. B Beam Interact. Mater. At.* **2019**, *451*, 113–121. [\[CrossRef\]](#)
10. Akel, F.Z.; Izerrouken, M.; Belgaid, M. Neutrons and swift heavy ions irradiation induced damage in SiC single crystal. *Mater. Today Commun.* **2023**, *37*, 107268. [\[CrossRef\]](#)
11. Kozlovskiy, A.; Kenzhina, I.; Alyamova, Z.A.; Zdorovets, M. Optical and structural properties of AlN ceramics irradiated with heavy ions. *Opt. Mater.* **2019**, *91*, 130–137. [\[CrossRef\]](#)
12. Zinkle, S.J.; Jones, J.W.; Skuratov, V.A. Microstructure of swift heavy ion irradiated SiC, Si<sub>3</sub>N<sub>4</sub> and AlN. *MRS Online Proc. Libr. (OPL)* **2000**, *650*, R3–R19. [\[CrossRef\]](#)
13. Glyva, V.; Natalia, K.; Nazarenko, V.; Burdeina, N.; Karaieva, N.; Levchenko, L.; Panova, O.; Tykhenko, O.; Khalmuradov, B.; Khodakovskyy, O. Development and study of protective properties of the composite materials for shielding the electromagnetic fields of a wide frequency range. *East.-Eur. J. Enterp. Technol.* **2020**, *2*, 104. [\[CrossRef\]](#)
14. Pikhay, E.; Roizin, Y.; Nemirovsky, Y. Ultra-low power consuming direct radiation sensors based on floating gate structures. *J. Low Power Electron. Appl.* **2017**, *7*, 20. [\[CrossRef\]](#)
15. Schrimpf, R.D.; Fleetwood, D.M. (Eds.) *Radiation Effects and Soft Errors in Integrated Circuits and Electronic Devices*; World Scientific: Singapore, 2004; Volume 34.
16. Malothu, R.; Rao, R.S. Combination of Copper Bismuth Oxide (CuBi<sub>2</sub>O<sub>4</sub>) and Polymer Composites from Plastic Waste: A Boon for EMF Shielding. *I-Manag. J. Future Eng. Technol.* **2021**, *16*, 11.
17. Awad, E.H.; Raslan, H.A.; Abou-Laila, M.T.; Taha, E.O.; Atta, M.M. Synthesis and characterization of waste polyethylene/Bi<sub>2</sub>O<sub>3</sub> composites reinforced with CuO/ZnO nanoparticles as sustainable radiation shielding materials. *Polym. Eng. Sci.* **2024**; early view.
18. Eren Belgin, E.; Aycik, G.A. Preparation and radiation attenuation performances of metal oxide filled polyethylene based composites for ionizing electromagnetic radiation shielding applications. *J. Radioanal. Nucl. Chem.* **2015**, *306*, 107–117. [\[CrossRef\]](#)
19. Cho, J.H.; Kim, M.S.; Rhim, J.D. Comparison of radiation shielding ratios of nano-sized bismuth trioxide and molybdenum. *Radiat. Eff. Defects Solids* **2015**, *170*, 651–658. [\[CrossRef\]](#)
20. Oğul, H.; Agar, O.; Bulut, F.; Kaçal, M.R.; Dilsiz, K.; Polat, H.; Akman, F. A comparative neutron and gamma-ray radiation shielding investigation of molybdenum and boron filled polymer composites. *Appl. Radiat. Isot.* **2023**, *194*, 110731. [\[CrossRef\]](#) [\[PubMed\]](#)
21. Abdolazadeh, T.; Morshedian, J.; Ahmadi, S. Preparation and characterization of nano WO<sub>3</sub>/Bi<sub>2</sub>O<sub>3</sub>/GO and BaSO<sub>4</sub>/GO dispersed HDPE composites for X-ray shielding application. *Polyolefins J.* **2022**, *9*, 73–83.
22. Seifert, N.; Slankard, P.; Kirsch, M.; Narasimham, B.; Zia, V.; Brookreson, C.; Vo, A.; Mitra, S.; Gill, B.; Maiz, J. Radiation-induced soft error rates of advanced CMOS bulk devices. In Proceedings of the 2006 IEEE International Reliability Physics Symposium Proceedings, San Jose, CA, USA, 26–30 March 2006.

23. Seifert, N.; Ambrose, V.; Gill, B.; Shi, Q.; Allmon, R.; Recchia, C.; Mukherjee, S.; Nassif, N.; Krause, J.; Pickholtz, J.; et al. On the radiation-induced soft error performance of hardened sequential elements in advanced bulk CMOS technologies. In Proceedings of the 2010 IEEE International Reliability Physics Symposium, Anaheim, CA, USA, 2–6 May 2010.
24. Kim, B.R.; Lee, H.K.; Kim, E.; Lee, S.H. Intrinsic electromagnetic radiation shielding/absorbing characteristics of polyaniline-coated transparent thin films. *Synth. Met.* **2010**, *160*, 1838–1842. [[CrossRef](#)]
25. Al-Balushi, M.A.; Ahmed, N.M.; Zyoud, S.H.; Mohammed Ali, M.K.; Akhdar, H.; Aldaghri, O.A.; Ibaouf, K.H. Ionization radiation shielding effectiveness of lead acetate, lead nitrate, and bismuth nitrate-doped zinc oxide nanorods thin films: A comparative evaluation. *Materials* **2021**, *15*, 3. [[CrossRef](#)] [[PubMed](#)]
26. Soğuksu, A.K.; Kerli, S.; Kavun, Y.; Alver, Ü. Synthesis and characterizations of Ce-doped ZnO thin films for radiation shielding. *Opt. Mater.* **2024**, *148*, 114941. [[CrossRef](#)]
27. Kadyrzhhanov, D.B.; Kaliyekperov, M.E.; Idinov, M.T.; Kozlovskiy, A.L. Study of the Structural, Morphological, Strength and Shielding Properties of CuBi<sub>2</sub>O<sub>4</sub> Films Obtained by Electrochemical Synthesis. *Materials* **2023**, *16*, 7241. [[CrossRef](#)] [[PubMed](#)]
28. Muthamma, M.V.; Bubbly, S.G.; Gudennavar, S.B.; Narendranath, K.S. Poly (vinyl alcohol)–bismuth oxide composites for X-ray and  $\gamma$ -ray shielding applications. *J. Appl. Polym. Sci.* **2019**, *136*, 47949. [[CrossRef](#)]
29. Eskalen, H.; Kavun, Y.; Kerli, S.; Eken, S. An investigation of radiation shielding properties of boron doped ZnO thin films. *Opt. Mater.* **2020**, *105*, 109871. [[CrossRef](#)]
30. AbuAlRoos, N.J.; Amin, N.A.B.; Zainon, R. Conventional and new lead-free radiation shielding materials for radiation protection in nuclear medicine: A review. *Radiat. Phys. Chem.* **2019**, *165*, 108439. [[CrossRef](#)]
31. Chan, T.-C.; Chueh, Y.-L.; Liao, C.-N. Manipulating the crystallographic texture of nanotwinned Cu films by electrodeposition. *Cryst. Growth Des.* **2011**, *11*, 4970–4974. [[CrossRef](#)]
32. Baskaran, I.; Sankara Narayanan, T.S.N.; Stephen, A. Pulsed electrodeposition of nanocrystalline Cu–Ni alloy films and evaluation of their characteristic properties. *Mater. Lett.* **2016**, *60*, 1990–1995. [[CrossRef](#)]
33. Otte, H.M. Lattice parameter determinations with an X-ray spectrometer by the debye-scherrer method and the effect of specimen condition. *J. Appl. Phys.* **1961**, *32*, 1536–1546. [[CrossRef](#)]
34. Ebrahimi, F.; Liscano, A.J.; Kong, D.; Krishnamoorthy, V. Evolution of texture in electrodeposited Ni/Cu layered nanostructures. *Philos. Mag.* **2003**, *83*, 457–476. [[CrossRef](#)]
35. Wu, K.-J.; Edmund, C.M.; Shang, C.; Guo, Z. Nucleation and growth in solution synthesis of nanostructures—from fundamentals to advanced applications. *Prog. Mater. Sci.* **2022**, *123*, 100821. [[CrossRef](#)]
36. Chauhan, K.V.; Rawal, S.K. A review paper on tribological and mechanical properties of ternary nitride based coatings. *Procedia Technol.* **2014**, *14*, 430–437. [[CrossRef](#)]
37. Liu, Z.; Ren, S.; Li, T.; Chen, P.; Hu, L.; Wu, W.; Li, S.; Liu, H.; Li, R.; Zhang, Y. A Comparison Study on the Microstructure, Mechanical Features, and Tribological Characteristics of TiN Coatings on Ti<sub>6</sub>Al<sub>4</sub>V Using Different Deposition Techniques. *Coatings* **2024**, *14*, 156. [[CrossRef](#)]
38. Wu, S.; Wu, S.; Zhang, G.; Zhang, W. Hardness and elastic modulus of titanium nitride coatings prepared by pirac method. *Surf. Rev. Lett.* **2018**, *25*, 1850040. [[CrossRef](#)]
39. Pujada, B.R.; Tichelaar, F.D.; Janssen, G.C.A.M. Hardness of and stress in tungsten carbide–diamond like carbon multilayer coatings. *Surf. Coat. Technol.* **2008**, *203*, 562–565. [[CrossRef](#)]
40. Bouzakis, K.-D.; Hadjiyiannis, S.; Skordaris, G.; Mirisidis, I.; Michailidis, N.; Efstathiou, K.; Pavlidou, E.; Erkens, G.; Cremer, R.; Rambadt, S.; et al. The effect of coating thickness, mechanical strength and hardness properties on the milling performance of PVD coated cemented carbides inserts. *Surf. Coat. Technol.* **2004**, *177*, 657–664. [[CrossRef](#)]
41. Ezzeldin, M.; Al-Harbi, L.M.; Sadeq, M.S.; Mahmoud, A.E.; Muhammad, M.A.; Ahmed, H.A. Impact of CdO on optical, structural, elastic, and radiation shielding parameters of CdO–PbO–ZnO–B<sub>2</sub>O<sub>3</sub>–SiO<sub>2</sub> glasses. *Ceram. Int.* **2023**, *49*, 19160–19173. [[CrossRef](#)]
42. Sayyed, M.I.; Rammah, Y.S.; Abouhaswa, A.S.; Tekin, H.O.; Elbashir, B.O. ZnO–B<sub>2</sub>O<sub>3</sub>–PbO glasses: Synthesis and radiation shielding characterization. *Phys. B Condens. Matter* **2018**, *548*, 20–26. [[CrossRef](#)]

**Disclaimer/Publisher’s Note:** The statements, opinions and data contained in all publications are solely those of the individual author(s) and contributor(s) and not of MDPI and/or the editor(s). MDPI and/or the editor(s) disclaim responsibility for any injury to people or property resulting from any ideas, methods, instructions or products referred to in the content.